Heinz Ulbricht Frank Schweitzer

Phase transitions in binary systems : theory and experiments

Rostock: Wilhelm-Pieck-Universität, 1988

https://purl.uni-rostock.de/rosdok/ppn1870256913

ISSN 0138–3140

Phase Transitions in Binary Systems: Theory and Experiments

ROSTOCKER
PHYSIKALISCHE
MANUSKRIPTE

Heft 12

Seit 1977 sind bisher 11 Rostocker Physikalische Manuskripte erschienen:

Heft 6: Die Rostocker Elektrolyt-Datenbank SAFE 1983

Heft 7: Strukturuntersuchungen an nichtkristallinen und partiell kristallinen Stoffen 1985

Heft 8: Nonlinear Irreversible Processes and Phase Transitions 1985

Heft 9: Klassische und Quantenstatistik dichter Systeme im Gleichgewicht und Nichtgleichgewicht - Stochastische Prozesse 1986

Heft 10: Thermodynamics and Kinetics of First-Order Phase Transitions 1987

Heft 11: Strukturuntersuchungen an nichtkristallinen und partiell kristallinen Stoffen 1987

Bezugsmöglichkeiten

- Bestellung aus der DDR über die Wilhelm-Pieck-Universität Rostock, Abt. Wissenschaftspublizistik, Vogelsang 13/14, Rostock, DDR - 2500.
- Bestellungen aus dem Ausland über die Firma Buchexport, Volkseigener Außenhandelsbetrieb der DDR, Leninstr. 16, Leipzig, DDR - 7010.

Ferner sind die Hefte im Rahmen des Schriftentausches über die Wilhelm-Pieck-Universität Rostock, Universitätsbibliothek, Tauschstelle, Universitätsplatz 5, Rostock, DDR - 2500, zu beziehen.

Rostocker Physikalische Manuskripte
Heft 12

PHASE TRANSITIONS IN BINARY SYSTEMS: THEORY AND EXPERIMENTS

Wilhelm-Pieck-Universität Rostock
Sektion Physik
1988

Herausgeber: Der Rektor der Wilhelm-Pieck-Universität Rostock

Wissenschaftliche Leitung: Prof. Dr. Heinz Ulbricht
Wissenschaftliche Bearbeitung: Dr. Frank Schweitzer
Herstellung der Druckvorlage: Hiltrud Bahlo

Redaktionsschluß: 1. 3. 1988

Zitat-Kurztitel: Rostock.Phys.Manuskr. (1988) 12

Wilhelm-Pieck-Universität Rostock
Abt. Wissenschaftspublizistik
Vogelsang 13/14, Telefon 369 577
Rostock, DDR - 2500
Genehmigungs-Nr.: C 100/88
Druck: Ostsee-Druck Rostock, Betriebsteil Ribnitz II-15-14·0.30
01100

Contents

Preface

Many areas of current interest in material sciences and its applications require an improved knowledge of the conditions for and the kinetics of first-order phase transitions. Thus, despite its long history, investigations of first-order phase transition remain an intensively developing field of research.

In continuation of earlier publications (see, e.g., Rostocker Physikalische Manuskripte 8 (1985), 10 (1987)) selected contributions of scientists of the Sektion Physik der Wilhelm-Pieck-Universität Rostock (WB I and WB IV) and colleagues from other institutes are presented in this booklet. The main topic of the common research activities, reflected here, is the process of nucleation and growth in multicomponent systems, in general, and binary systems, in particular. These processes are described here both from experimental and theoretical points of view.

We hope that the scientific results outlined will have a practical importance for applications in material sciences and that this booklet will contribute to an intensive interchange of ideas.

We thank Mrs. Hiltrud Bahlo, who typed the whole manuscript in a perfect way, again, and Mrs. Renate Nareyka and Mrs. Christine Benkißer for preparing the figures.

Heinz Ulbricht Frank Schweitzer

Rostocker Physikalische Manuskripte, Heft 12 (1988)

Jürn Schmelzer; Iwan Gutzow; Radost Pascova

On the Theoretical Description of the Influence of Elastic Strains on the Process of Crystallization in Glasses

1. Introduction

Usually the process of formation and growth of a new phase in solids, in general, and binary solid solutions, in particular, is accompanied by the development of elastic strains due to the evolution of the new phase /1/. These elastic strains modify the kinetics of growth, they may lead to a stop of the growth or prevent the formation of the new phase et al. /2,3/. Thus, a possibly adequate and at the same time sufficiently simple theoretical description of the evolving elastic strains is required to allow a comparison with experimental investigations. In particular, it is of interest to study, how the size of the system influences the process of formation of elastic strains and, consequently, the kinetics of the transition.

Based on such arguments, in the following paragraphs two basic models for a description of elastic strains, evolving in phase transformations in solids, are analyzed. The calculations are carried out at a sufficiently general level. As far as this may be required for applications not only the final but also intermediate results are given explicitely.

Hereby we restrict ourselves to the case of isotropic and homogeneous media, where the elastic properties can be described by two constants, the Young modulus E and the Poisson number σ. The results should allow a qualitative understanding of the influence of elastic strains on phase transformations also for the case of anisotropic media, if not the effects due to the anisotropy are the aim of the investigation /4/. Moreover, the influence of surface effects on the evolution of the elastic strains is not taken into account explicitely. If necessary, this can be done by an appropriate redefinition of the external pressure.

2. General Solutions of the Equation of the Linear Theory of Elasticity in the Case of Spherical Symmetry

The basic equations of the theory of elasticity for the calculation of the vector of deformation $\bar{u}$ has in the absence of volume forces the following form /5/:

$$\text{grad}(\text{div}\,\bar{u}) = 0 \tag{2.1}$$

Due to the spherical symmetry only the radial component of the vector of deformation u_r is different from zero, it is determined by

$$\frac{1}{r^2}\frac{\partial}{\partial r}(r^2 u_r) = 3C_1 \qquad C_1 \text{ - constant} \tag{2.2}$$

with the general solution

$$u_r = C_1 r + C_2/r^2 \qquad C_2 \text{ - constant} \tag{2.3}$$

The constants C_1 and C_2 have to be determined from the boundary conditions. They reflect the specific properties of the system under consideration.

The comprehensive description of the state of deformation requires the knowledge of the components of the tensor of deformation U_{ik} and the stress tensor σ_{ik}. In spherical coordinates they read /5/:

$$\begin{aligned}
&U_{rr} = C_1 - 2C_2/r^3 \qquad U_{\vartheta\vartheta} = U_{\varphi\varphi} = C_1 + C_2/r^3 \\
&U_{r\varphi} = U_{\vartheta\varphi} = U_{r\vartheta} = 0 \qquad \sigma_{r\varphi} = \sigma_{\vartheta\varphi} = \sigma_{r\vartheta} = 0 \\
&\sigma_{rr} = C_1 \frac{E}{1-2\sigma} - C_2 \frac{2E}{1+\sigma}\frac{1}{r^3} \\
&\sigma_{\vartheta\vartheta} = \sigma_{\varphi\varphi} = C_1 \frac{E}{1-2\sigma} + C_2 \frac{E}{1+\sigma}\frac{1}{r^3}
\end{aligned} \tag{2.4}$$

The work per unit volume or the density of free energy f (the temperature is assumed to be constant) of the elastically deformed state, described by eqs. (2.4), is generally given by /5/

$$f = \frac{E}{2(1+\sigma)}\left[U_{ik}U_{ik} + \frac{\sigma}{1-2\sigma}(U_{ll})^2\right] \tag{2.5}$$

Here the sum convention is used.
For spherical symmetry we get as a special case

$$f = \frac{E}{2(1+\sigma)}\left[U_{rr}^2 + U_{\vartheta\vartheta}^2 + U_{\varphi\varphi}^2 + \frac{\sigma}{1-2\sigma}\,(U_{rr}+U_{\varphi\varphi}+U_{\vartheta\vartheta})^2 \right] \qquad (2.6)$$

and after substitution of eqs. (2.4) into eq. (2.6)

$$f = \frac{3E}{2(1+\sigma)}\left[C_1^2\,\frac{1+\sigma}{1-2\sigma} + \frac{2C_2^2}{r^6} \right] \qquad (2.7)$$

In the following paragraph the constants C_1 and C_2 are determined for different boundary conditions which are of relevance for the considered subsequently models of evolution of elastic strains.

3. Determination of the Constants from the Boundary Conditions

3.1. Deformation of a Sphere

For the case of the deformation of a sphere with the radius R the constants of integration are determined by the boundary conditions (see also /6/)

$$u_r(r=0) = 0 \qquad \sigma_{rr}(r=R) = -p \qquad (3.1)$$

As the result one obtains

$$C_2 = 0 \qquad C_1 = -p\,\frac{1-2\sigma}{E} \qquad (3.2)$$

where p is the external pressure on the sphere, which gives rise to the deformation.

An alternative definition of C_1 is possible through the variation of the volume ΔV due to the external pressure. Since the relative variation of the volume resulting from the elastic deformations is given by /5/

$$\frac{d(V'-V)}{dV} = \operatorname{div}\vec{u} = U_{rr} + U_{\varphi\varphi} + U_{\vartheta\vartheta} \qquad (3.3)$$

an integration over the whole volume yields

$$C_1 = \frac{1}{3}\,\frac{\Delta V}{V} \qquad (3.4)$$

Thus, a comparison between eqs. (3.2) and (3.4) leads to

$$-p\,\frac{1-2\sigma}{E} = \frac{1}{3}\,\frac{\Delta V}{V} \qquad (3.5)$$

which interconnects the external pressure with variations of the volume of the sphere.

3.2. Deformation of a Centred Hollow Sphere

We consider as a second special case the deformation of a centred hollow sphere with the inner radius R_1 and the outer radius R_2. The possible boundary conditions and the resulting expressions for the constants C_1 and C_2 are given below. In these equations ΔR_i denotes the variation of the inner or outer radius of the hollow sphere, respectively.

$$\sigma_{rr}(R_2) = -p_2 \qquad u_r(R_1) = \Delta R_1$$

$$C_1 = \frac{1-2\sigma}{E} \; \frac{2ER_1^2 \Delta R_1 - R_2^3 p_2 (1+\sigma)}{(1+\sigma)R_2^3 + 2(1-2\sigma)R_1^3} \tag{3.6}$$

$$C_2 = R_1^2 R_2^3 \frac{1+\sigma}{E} \; \frac{p_2 R_1 (1-2\sigma) + E \Delta R_1}{(1+\sigma)R_2^3 + 2(1-2\sigma)R_1^3}$$

$$\sigma_{rr}(R_1) = -p_1 \qquad u_r(R_2) = \Delta R_2$$

$$C_1 = \frac{(1-2\sigma)\left[2ER_2^2 \Delta R_2 - p_1 (1+\sigma)R_1^3\right]}{E\left[(1+\sigma)R_1^3 + 2(1-2\sigma)R_2^3\right]} \tag{3.7}$$

$$C_2 = \frac{R_1^3 (1+\sigma)\left[ER_2^2 \Delta R_2 + p_1 (1-2\sigma)R_2^3\right]}{E\left[(1+\sigma)R_1^3 + 2(1-2\sigma)R_2^3\right]}$$

$$u_r(R_1) = \Delta R_1 \qquad u_r(R_2) = \Delta R_2$$

$$C_1 = \frac{1}{R_2^3 - R_1^3}\left[R_2^2 \Delta R_2 - R_1^2 \Delta R_1\right] \qquad C_2 = \frac{R_1^3 R_2^3}{R_2^3 - R_1^3}\left[\frac{\Delta R_1}{R_1} - \frac{\Delta R_2}{R_2}\right] \tag{3.8}$$

$$\sigma_{rr}(R_1) = -p_1 \qquad \sigma_{rr}(R_2) = -p_2$$

$$C_1 = \frac{1-2\sigma}{E(R_2^3-R_1^3)}\left[p_1R_1^3-p_2R_2^3\right] \qquad C_2 = -\frac{(1+\sigma)(p_2-p_1)R_1^3R_2^3}{2E(R_2^3-R_1^3)} \tag{3.9}$$

These expressions are simplified if special or limiting cases are considered, e.g., $R_2 \rightarrow \infty$.

4. Elastic Strains in Recrystallization Processes

The first model of evolution of elastic strains, analyzed here, is based on the following considerations.

Let us assume that in the centre of an approximately spherical body with the radius R_2 and the elastic constants E_2 and σ_2 a spherical cluster of a new phase with the constants E_1 and σ_1 is formed. In the absence of elastic strains the cluster is characterized by a radius R and a volume V.

The mean volume per particle in both phases is denoted by $v^{(2)}$ and $v^{(1)}$, respectively. Introducing the partial molar volumes v_i and the molar fractions of the components x_i, these quantities can be written as /7/

$$v^{(1)} = \sum_{i=1}^{n} x_i^{(1)}v_i^{(1)} \qquad v^{(2)} = \sum_{i=1}^{n} x_i^{(2)}v_i^{(2)} \tag{4.1}$$

for the different phases, specified by the superscripts (1) and (2). n is the number of components.

For perfect mixtures v_i can be replaced by v_{io}, the volume per particle of the pour components in the different phases /7/.

If $v^{(1)} \neq v^{(2)}$, the crystallization results in a variation of the volume of the part of the matrix, which undergoes the transformation. In the absence of elastic strains, this variation would be equal to

$$\Delta V_t = V\delta \quad \text{with} \quad \delta = (v^{(2)}-v^{(1)})/v^{(1)} \tag{4.2}$$

If the cluster remains in contact with the surrounding mother phase in the course of crystallization, which is assumed in the following, then elastic strains occur.

According to eqs. (2.3), (2.4), (3.2) and (3.4) for the

cluster phase these strains are described by

$$U_{rr} = U_{\vartheta\vartheta} = U_{\varphi\varphi} = C_1^{(1)} \qquad u_r = C_1^{(1)} r \qquad C_1^{(1)} = \frac{1}{3}\frac{\Delta V}{V}$$
$$\sigma_{rr} = \sigma_{\vartheta\vartheta} = \sigma_{\varphi\varphi} = C_1^{(1)} \frac{E_1}{1-2\sigma_1} \qquad \sigma_{ik} = U_{ik} = 0, \quad i \neq k \tag{4.3}$$

for the matrix we obtain in a similar way

$$U_{rr} = C_1^{(2)} - \frac{2C_2^{(2)}}{r^3} \qquad U_{\vartheta\vartheta} = U_{\varphi\varphi} = C_1^{(2)} + \frac{C_2^{(2)}}{r^3}$$
$$\sigma_{rr} = C_1^{(2)} \frac{E_2}{1-2\sigma_2} - C_2^{(2)} \frac{2E_2}{1+\sigma_2} \frac{1}{r^3} \tag{4.4}$$
$$\sigma_{\vartheta\vartheta} = \sigma_{\varphi\varphi} = C_1^{(2)} \frac{E_2}{1-2\sigma_2} + C_2^{(2)} \frac{E_2}{1+\sigma_2} \frac{1}{r^3}$$
$$C_1^{(2)} = \frac{2(1-2\sigma_2)R_1^2 \Delta R_1}{(1+\sigma_2)R_2^3+2(1-2\sigma_2)R_1^3} \qquad C_2^{(2)} = \frac{R_2^3(1+\sigma_2)R_1^2 \Delta R_1}{(1+\sigma_2)R_2^3+2(1-2\sigma_2)R_1^3}$$

It is assumed here that the outside pressure on the matrix is equal to zero and the boundary conditions (3.6) are applied.

If one denotes the inner radius of the hollow sphere and the radius of the newly formed spherical phase both in the elastically deformed state by R', then the condition of the mechanical equilibrium at the interface is given by

$$\sigma_{rr}^{(1)}(R') = \sigma_{rr}^{(2)}(R') \tag{4.5}$$

or by

$$\frac{2R_1^2 \Delta R_1 E_2}{(1+\sigma_2)R_2^3+2(1-2\sigma_2)R_1^3} \left(1 - \frac{R_2^3}{R_1^3}\right) = \frac{E_1}{(1-2\sigma_1)} \frac{1}{3}\frac{\Delta V}{V} \tag{4.6}$$

In eq. (4.6) $(1-R_2^3/(R')^3)$ was replaced by $(1-R_2^3/R_1^3)$ which is possible due to the smallness of the elastic deformations. Similar approximations are used in the derivation of eqs. (4.8) and (4.12).

The total variation of the volume ΔV_t is in the deformed state compensated by a change in the volume of the cluster ΔV and a variation of the inner radius of the hollow sphere ΔR_1. Thus we get

$$\Delta V - 4\pi R_1^2 \Delta R_1 = \delta V \qquad (4.7)$$

Eqs. (4.6) and (4.7) represent a system of two equations for the determination of ΔR_1 and ΔV and, consequently, of the constants $C_i^{(j)}$, i,j=1,2. Introducing the notation

$$B = 3\left[(1-2\sigma_1)\, 2E_2(R_2^3-R_1^3) + E_1\left[(1+\sigma_2)R_2^3+2R_1^3(1-2\sigma_2)\right]\right] \qquad (4.8)$$

one obtains

$$\frac{\Delta V}{V} = \frac{6\delta}{B}(1-2\sigma_1)E_2(R_2^3-R_1^3) \qquad (4.9)$$

$$\Delta R_1 = -\frac{\delta}{B} E_1 R_1\left[(1+\sigma_2)R_2^3+2(1-2\sigma_2)R_1^3\right]$$

The constants $C_i^{(j)}$ are given, consequently, as

$$C_1^{(1)} = \frac{\delta}{B} 2E_2(1-2\sigma_1)(R_2^3-R_1^3) \qquad (4.10)$$

$$C_1^{(2)} = -\frac{\delta}{B} 2E_1R_1^3(1-2\sigma_2) \qquad C_2^{(2)} = -\frac{\delta}{B}E_1R_1^3R_2^3(1+\sigma_2)$$

A substitution of these results into eq. (2.7) yields the following expressions for the density of energy of elastic deformations f in both phases

$$f^{(1)} = 6E_1E_2^2(1-2\sigma_1)(R_2^3-R_1^3)^2\frac{\delta^2}{B^2} \qquad (4.11)$$

$$f^{(2)} = 6(1-2\sigma_2)E_1^2E_2R_1^6\frac{\delta^2}{B^2}\left(1+\frac{R_2^6}{r^6}\frac{1+\sigma_2}{(1-2\sigma_2)}\right)$$

Integration over the whole volume results in the total energy of elastic deformations F connected with the evolution of a cluster of the volume V

$$F^{(1)} = 6E_1E_2^2(1-2\sigma_1)(R_2^3-R_1^3)^2\frac{\delta^2}{B^2}V \qquad (4.12)$$

$$F^{(2)} = 6(1-2\sigma_2)E_1^2E_2R_1^3\left\{R_2^3-R_1^3-\frac{1+\sigma_2}{2(1-2\sigma_2)}R_2^6\left[\frac{1}{R_2^3}-\frac{1}{R_1^3}\right]\right\}\frac{\delta^2}{B^2}V$$

$$F = F^{(1)} + F^{(2)}$$

In the limiting case $R_2 \to \infty$ these expressions are reduced to

$$F^{(1)} = \frac{2}{3} \frac{E_1 E_2^2 (1-2\sigma_1)}{\left[2E_2(1-2\sigma_1)+E_1(1+\sigma_2)\right]^2} \delta^2 v$$

$$F^{(2)} = \frac{E_2 E_1^2 (1+\sigma_2)}{3\left[2E_2(1-2\sigma_1)+E_1(1+\sigma_2)\right]^2} \delta^2 v \qquad (4.13)$$

$$F = \frac{E_1 E_2}{3\left[2E_2(1-2\sigma_1)+E_1(1+\sigma_2)\right]} \delta^2 v$$

As can be verified easily from eqs. (4.12) this limiting case is realized in a good approximation for $R_2 \gtrsim 5R_1$. Vice versa, finite size effects connected with elastic strains are of importance only for $R_2 \lesssim 5R_1$.

If, in particular, the elastic constants of both phases are nearly the same, then eq. (4.13) is further reduced to an expression, derived already by Nabarro /8/.

$$F = \frac{E}{9(1-\sigma)} \delta^2 v \qquad (4.14)$$

The calculations outlined here are more general, compared with Nabarro's results, since, first, the possibility of different elastic constants of both phases is taken into account, and, second, in a simple form the dependence of the evolving elastic strains on the size of the system is reflected.

The considered here model for the evolution of elastic strains is applicable both for crystallization and segregation processes /1/, if the evolving strains are due mainly to differences in the volume per particle in both considered phases ($F \sim \delta^2$ in eq. (4.12)). There exist, however, situations where the strains are due to other mechanisms. One of these mechanisms is analyzed in paragraph 5.

5. Segregation in Binary Solid Solutions. A Second Model for the Description of Elastic Strains

Let us assume, that due to segregation processes of one of the components a spherical cavity in a solid elastic matrix is filled by a newly evolving phase. The initial radius of the ca-

vity and thus of the cluster is denoted by R_1.

Due to the thermodynamic driving force of the segregation process the cluster will continue the growth also for a certain range of values of its radius $R > R_1$, until the driving force is compensated eventually by the elastic strains.

The calculation of the free energy of elastic deformations for the considered, now, mechanism is carried out, again, under the additional assumption, that the cavity with the radius R_1 is located in the centre of a spherical matrix with the radius R_2. This assumption allows a simple estimation of finite size effects also for this second case.

The further growth of the cluster for $R \gtrsim R_1$ is connected with an increase of the inner radius of the matrix ΔR_1. Thus, for the determination of the state of deformation of the matrix we have to apply the boundary conditions (3.6) and with $p_2=0$ we get

$$C_1^{(2)} = \frac{2(1-2\sigma_2)R_1^2 \Delta R_1}{(1+\sigma_2)R_2^3+2(1-2\sigma_2)R_1^2} \tag{5.1}$$

$$C_2^{(2)} = R_1^2 R_2^3 \frac{(1+\sigma_2)\Delta R_1}{(1+\sigma_2)R_2^3+2(1-2\sigma_2)R_1^3}$$

According to eq. (2.7) the density of energy of elastic deformations for the matrix is given then as

$$f^{(2)} = \frac{6E_2(1-2\sigma_2)(R_1^2 \Delta R_1)^2}{\left[(1+\sigma_2)R_2^3+2(1-2\sigma_2)R_1^3\right]^2} \left(1+ \frac{R_2^6}{r^6} \frac{1+\sigma_2}{2(1-2\sigma_2)}\right) \tag{5.2}$$

From the equilibrium condition at the interface

$$\sigma_{rr}^{(2)}(R') = \sigma_{rr}^{(1)}(R') = - p \tag{5.3}$$

the constant $C_1^{(1)}$ is determined as (see eqs. (3.2) and (2.4))

$$C_1^{(1)} = \sigma_{rr}^{(2)}(R') \frac{1-2\sigma_1}{E_1} \tag{5.4}$$

$$C_1^{(1)} = \frac{2E_2(1-2\sigma_1)R_1^2 \Delta R_1}{E_1\left[(1+\sigma_2)R_2^3+2(1-2\sigma_2)R_1^3\right]} \left(1- \frac{R_2^3}{R'^3}\right)$$

Consequently, the expression for $f^{(1)}$ reads

$$f^{(1)} = \frac{6E_2^2(1-2\sigma_2)(R_1^2\Delta R_1)^2}{E_1\left[(1+\sigma_2)R_2^3+2(1-2\sigma_2)R_1^3\right]^2}\left(1-\frac{R_2^3}{R'^3}\right)^2 \qquad (5.5)$$

To obtain the total energy of elastic deformations one has to carry out an integration of f over the whole volume in the undeformed state /5/. Denoting by R^+ the radius of the cluster in the absence of elastic strains one obtains

$$F^{(1)} = 4\pi\int_0^{R^+} f^{(1)}r^2dr = \frac{4\pi}{3}f^{(1)}(R^+)^3 \qquad (5.6)$$

But since the deformations are small we may replace $R^+ \simeq R' \simeq R_1$ and eq. (5.6) is transformed in a good approximation into

$$F^{(1)} = \frac{6E_2^2(1-2\sigma_2)(R_1^2\Delta R_1)^2(R_2^3-R_1^3)^2}{E_1\left[(1+\sigma_2)R_2^3+2(1-2\sigma_2)R_1^3\right]^2R_1^3}\frac{4\pi}{3} \qquad (5.7)$$

For the matrix a similar approach yields

$$F^{(2)} = 4\pi\int_{R_1}^{R_2} f^{(2)}r^2dr \qquad (5.8)$$

$$F^{(2)} = \frac{6E_2(1-2\sigma_2)(R_1^2\Delta R_1)^2}{\left[(1+\sigma_2)R_2^3+2(1-2\sigma_2)R_1^3\right]^2}\frac{4\pi}{3}\left(R_2^3-R_1^3-\frac{(1+\sigma_2)R_2^3}{2(1-2\sigma_2)}\left(1-\frac{R_2^3}{R_1^3}\right)\right)$$

Both terms $F^{(1)}$ and $F^{(2)}$ are proportional to $(R_1^2\Delta R_1)^2$, where by R_1 the inner radius of the hollow sphere and the initial radius of the cluster were denoted, for which strains of the considered type start to develop. Consequently, also the total energy of elastic deformations F is determined by this term.

$$F = \frac{2E_2(1-2\sigma_2)(R_1^2\Delta R_1)^2(R_2^3-R_1^3)4\pi}{\left[(1+\sigma_2)R_2^3+2(1-2\sigma_2)R_1^3\right]^2}\left[\frac{E_2}{E_1}\frac{R_2^3-R_1^3}{R_1^3}+1+\frac{(1+\sigma_2)R_2^3}{2(1-2\sigma_2)R_1^3}\right] \qquad (5.9)$$

But at the same time

$$4\pi R_1^2\Delta R_1 = \Delta V \qquad (5.10)$$

ΔV being the increase of the volume of the cluster in the course of its growth from R_1 to $R_1+\Delta R_1$. Introducing the nota-

tion $V_o = 4\pi R_1^3/3$ eq. (5.9) yields

$$F = \frac{2E_2(1-2\sigma_2)(R_2^3-R_1^3)}{3\left[(1+\sigma_2)R_2^3+2(1-2\sigma_2)R_1^3\right]^2}\left[\left[\frac{E_2}{E_1}(R_2^3-R_1^3)+R_1^3+\frac{(1+\sigma_2)R_2^3}{2(1-2\sigma_2)}\right]\frac{(\Delta V)^2}{V_o}\right] \tag{5.11}$$

In the limiting case $R_2 \to \infty$ this equation is simplified to

$$F = \frac{E_2\left[2E_2(1-2\sigma_2)+E_1(1+\sigma_2)\right]}{3(1+\sigma_2)^2 E_1}\frac{(\Delta V)^2}{V_o} \tag{5.12}$$

If, further, the elastic constants of both phases are nearly the same, eq.(5.12) reads

$$F = \frac{E(1-\sigma)}{(1+\sigma)^2}\frac{(\Delta V)^2}{V_o} \tag{5.13}$$

6. Discussion

The main difference between the results obtained for both models of evolution of elastic strains consists in the following: While in the first case the elastic strains grow proportional to the volume of the new phase, in the second one F is proportional to $(V-V_o)^2$. Such a different behaviour can be expected to lead to a quite different growth kinetics.

It has been proven /2,3,6/, that this is, indeed, the case. For strains $F \sim V$ elastic strains result effectively only in a decrease of the thermodynamic driving force of the phase transition. Once the transition is started it cannot be stopped by this type of strains. However, strains of the second type $F \sim (V-V_o)^2$ will always result in a stop of the growth for a sufficiently large size of the new phase. These conclusions are valid both for independent growth of the clusters and for the process of Ostwald ripening /2,3,6/.

The calculations, carried out here, can be generalized to model the evolution of elastic strains in crystallization processes from inner and outer surfaces. First steps in this direction have been undertaken (see /6,9,10/). A comprehensive analysis including the detailed discussion of finite size effects on the

process of crystallization under the influence of elastic strains will be presented later.

References

1. Christian, J.W.: The Theory of Transformation in Metals and Alloys, Oxford 1975
2. Schmelzer, J.; Gutzow, I.: Wiss.Z.WPU Rostock NR, Heft 4, 35 5; Z.Phys.Chem.(Leipzig) 269 (1988) ; "Ostwald Ripening in Viscoelastic Media", in: Springer Series in Synergetics, Eds. W. Ebeling; H. Ulbricht, vol. 33, page 144
3. Schmelzer, J.; Gutzow, I.; Pascova, R.: Kinetics of Segregation in Elastic and Viscoelastic Media, to be published
4. Skripov, V.P.; Koverda, V.P.: Spontaneous Crystallization of Undercooled Liquids, Moscow 1984 (in Russian)
5. Landau, L.D.; Lifshitz, E.M.: Elastizitätstheorie, Berlin 1976
6. Schmelzer, J.: Thermodynamik finiter Systeme und die Kinetik von thermodynamischen Phasenübergängen 1. Art, Diss. B, Rostock 1985
7. Haase, R.: Thermodynamik der Mischphasen, Berlin 1956
8. Nabarro, F.R.N.: Proc.Phys.Soc. 52 (1940) 90; Proc.Roy.Soc. A 175 (1940) 519
9. Hoell, A.; Schmelzer, J.; Mahnke, R.: Wiss.Z.WPU Rostock,NR Heft 4, 35 (1986) 28
10. Hoell, A.: Belegarbeit, Diplomarbeit, Sektion Physik der WPU Rostock, 1985, 1986

Authors:

Dr. Jürn Schmelzer
Wilhelm-Pieck-Universität Rostock
Sektion Physik
Universitätsplatz 3
Rostock
DDR - 2500

Prof. Dr. Iwan Gutzow, Dr. Radost Pascova
Institute of Physical Chemistry
Bulgarian Academy of Sciences
Sofia
BG - 1040

Rostocker Physikalische Manuskripte, Heft 12 (1988)

Ulrich Lembke; Wolfhart Göcke; Winfried Blau

Experimental Investigation of Nucleation, Growth and Ripening in Photochromic Glasses

1. Introduction

Glasses on the basis of borosilicates containing metal halide microcrystallites are the foundation of the production of photochromic glasses. The photochromic effect of darkening during irradation with ultraviolet light and fading afterwards is caused by the properties of the microcrystallites precipitated in the glass owing to a heat treatment. In some glasses a liquid-liquid phase separation of the base glass is necessary in order to precipitate the metal halide within the minor phase of the glass. In the glasses investigated here the formation of the metal halide phase was shown to take place without any preceding phase separation of the glass /1/.

The photochromic properties of the glasses are strongly influenced by the structure properties of the microcrystallites (crystal structure, composition, diameter distribution, phase volume, number of crystallites per volume (particle density)). These parameters can be controlled by the heat treatment of the glass. Small Angle X-ray Scattering (SAXS) is an important tool for the investigation of the correlations between the conditions of the heat treatment and the structure properties. The results are used for the optimization of the production process of photochromic glasses.

2. Experimental

The SAXS technique is very useful in investigating sub-microscopic composition heterogeneities. In particular, the size distribution, the shape, the phase volume, the total inner surface and the particle density of a system of dispersed particles can be determined. In the case of phase separation in glasses

particles of spherical shape are formed. For a system of homogeneous spheres the particle diameter distribution $N^*(D)$ is /2/

$$N^*(D) = -\frac{d}{dr}\left[\frac{d^2C(r)}{dr^2}/r\right] \quad , \tag{1}$$

where D is the diameter of the sphere and C(r) is the correlation function. C(r) is calculated from the measured scattering curve by a transform technique based on both the Hankel transformation and the sampling theorem of the information theory /3,4/. The phase volume w of the dispersed particles can be calculated according to (2)

$$C(0) = w(1-w)\,(\Delta\varrho)^2 \quad , \tag{2}$$

where $\Delta\varrho$ is the difference of the electron density between the particle and the surrounding glass. $\Delta\varrho$ was determined by the means of X-ray diffraction investigations of the photochromic glasses which contain the precipitated light-sensitive microcrystallites.

The calculated distributions $N^*(D)$ were normalized in such a manner that the total volume of all particles together is equal to the volume fraction w:

$$N(D) = \frac{N^*(D)w}{\pi/6\int_0 D^3N^*(D)dD} \quad . \tag{3}$$

That means that the particle density is represented by the area under N(D).

The SAXS curves were obtained using a Kratky-camera with a step scanning device (Cu K_α radiation). The errors of the calculated structure functions N(D) resulting from the statistical errors of the recorded scattering intensities were estimated by a special procedure described in /4/.

Four photochromic glasses with different compositions were investigated. The Na_2O- Li_2O- K_2O- Al_2O_3- B_2O_3- SiO_2 glasses with an admixture of metal halide were heat treated at $T=610^oC$ in order to precipitate liquid droplets of the metal halide which become photoactive after the crystallization during the cooling of the glass. The batch compositions of the glasses I

and II differed in the halide composition (I: AgBr, II: $AgBr_{0,36}Cl_{0,64}$). The glasses III and IV were melted with an admixture of fluorine and a higher content of alkali oxides. In glass III $AgBr_{0,53}Cl_{0,47}$ particles were precipitated, glass IV contained microcrystallites of CuBr.

3. Results and discussion

For glass I, the evolution of the diameter distribution with increasing time of the heat treatment is shown in Fig. 1 and Fig. 2, respectively.

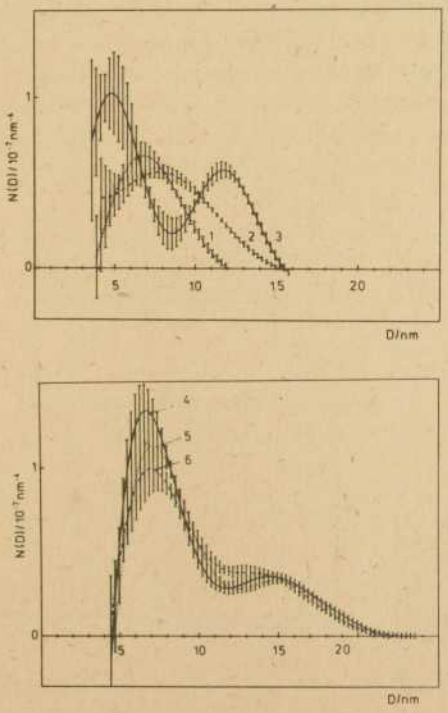

Fig. 1,2:
The diameter distribution functions of glass I, T=610°C, treatment times t:
1 - 0,5 h
2 - 1,0 h
3 - 1,5 h
4 - 2,0 h
5 - 4,0 h
6 - 8,0 h

Fig. 1 demonstrates that two generations of particles with different diameters grew independently for $t < 2$ h. The formation of two distinct generations of nuclei can be interpreted by the

thermal history of the glass. The temperature region of the maximum rate of the nucleus formation was passed two times, i.e. at the cooling procedure from the temperature of melting down to the room temperature and during the following heat treatment. Consequently, the nuclei that were already formed during cooling were in the stage of particle growth when the nucleation of a new particle generation took place during the heating of the glass.

For $t < 2$ h, the crystallites grew according to a reaction-limited growth mechanism /5,6/ indicated by the fact that $\bar{D} \sim t$, where $\bar{D}$ is the mean of N(D), and $w \sim t^3$ obtained by the aid of (2). For $t \geq 2$ h, the phase volume w remains constant and the growth law of $D^3 \sim t$ is valid (see Fig. 5). The smallest crystallites are dissolved. This is shown by the decreasing area under the peak of the smaller particles that indicates a diminution of the number of particles of this generation (Fig. 2). Thus it can be concluded that the stage of coarsening by ripening /7,8/ was reached.

The same ripening process was observed in the other glasses, too. For example it is indicated by the evolution of the volume distribution function of glass III with increasing treatment time (Fig. 3).

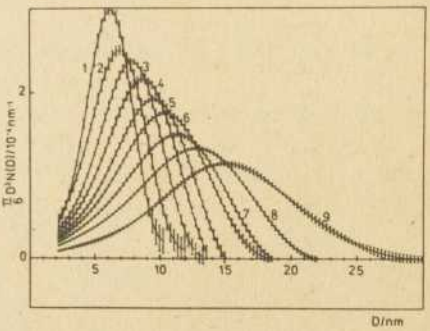

Fig. 3:
The volume distribution functions $\pi/6\ D^3N(D)$ of glass III, T=610°C
1 - 0,25 h 6 - 3,0 h
2 - 0,5 h 7 - 4,0 h
3 - 1,0 h 8 - 8,0 h
4 - 1,5 h 9 - 16,0 h
5 - 2,0 h

The fact that w = constant for $t \geq 0{,}25$ h is demonstrated, since the area under the volume distributions remains constant. The transport of material from the dissolving small particles to the

growing large particles results in a decreasing phase volume at smaller diameters and in an increasing phase volume at larger D for the same amount (compare the area differences left and right between two consecutive treatment states, Fig. 3).

The evidence for the existence of a diffusion-limited ripening mechanism is given in Fig. 4. The evolution of the particle density in dependence on the ripening time t according to (4) /8/

$$N(t) = N(t_o)\left\{1 + (t-t_o)\text{const}\right\}^{-1} \quad , \qquad (4)$$

where t_o is the beginning of the ripening, is shown in Fig. 4, where the sloped of the curves in logarithmic scales are equal to 1. This is consistent with the time dependence of the mean diameter of the particle system that ripen according to (5) /8/

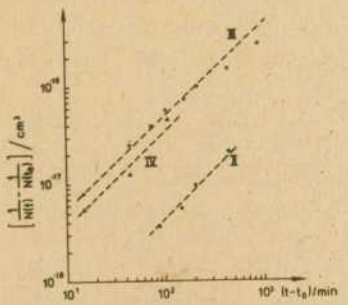

Fig. 4:
The evolution of the reciprocal particle densities during the ripening process, logarithmic scales

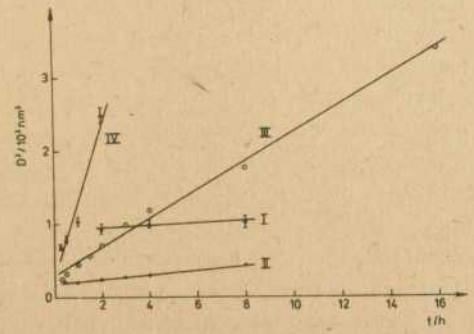

Fig. 5:
The dependence of the cubed mean diameter on the ripening time

$$\bar{D}^3(t) - \bar{D}^3(t_o) = \frac{64\,\sigma\,D_D\,c_o\,V_m^2}{9\,\nu\,R\,T}\,(t-t_o) \quad . \qquad (5)$$

This dependence is demonstrated in Fig. 5.

Using a stoichiometric factor $\nu = 1$ /8/, the molar volumes V_m at the absolute temperature T of the heat treatment /9/ and the results of measurements of the interfacial tension in this temperature region (0,20 ... 0,23 Nm^{-1}) /1/ the diffusion coefficients D_D were calculated from the slopes in Fig. 5. The solubility c_o was estimated by equation (6)

$$c_o = \frac{c\,d}{M} - \frac{w}{V_m} \quad , \qquad (6)$$

where the symbol c is the total concentration of silver or copper in the glass, M is the corresponding molar weight and w and V_m are the experimentally determined phase volume and the molar volume; d is the glass density at the treatment temperature. The calculated diffusion coefficients are given in the following table:

glass	I	II	III	IV
D_D / $10^{-4} m^2 s^{-1} (= cm^2 s^{-1})$	$3{,}1\ 10^{-15}$	$1{,}1\ 10^{-14}$	$2{,}5\ 10^{-13}$	$1{,}6\ 10^{-13}$

The obtained diffusion coefficients for the glasses III and IV correspond to the data given in /10/ for the diffusion of silverhalide in different glassforming melts near the glass temperature T_g. The missing fluorine in the batch material should be the reason for the smaller diffusion coefficients in the glasses I and II. Fluorine is known to decrease the viscosity of the melt. Therefore the fuorine addition together with the higher content of network modifiers (alkali ions) resulted in a higher diffusion mobility in the glasses III and IV in relation to the glasses I and II. These requirements on the glass composition have to be considered in the production of photochromic glasses. Moreover the lost of the metal halides during the melting can be reduced by a small content of fluorine, because it considerably

reduces the melting temperature.

In the investigated glasses particle densities of $7 \cdot 10^{14} \ldots 2 \cdot 10^{16}$ cm^{-3} were determined by SAXS at the beginning of the ripening. This is comparable with the experimental data given in /11/ for the precipitation of silverchloride particles in a sodium borate glass melt ($T \approx T_g$). In order to discuss the kinetics of the nucleation in our glasses some thermodynamical parameters were estimated.

According to the classical theory /12/ the steady-state homogeneous nucleation rate J can be expressed as a function of T by

$$J = K \exp\left(-(A_D + A_K)/kT\right) , \qquad (7)$$

where K is a constant, approximately independent of the temperature T, k is Boltzmann's constant and A_D and A_K are the energies of activation of the diffusion and the formation of a critical nucleus, respectively. For nuclei of spherical shape A_K is calculated by

$$A_K = \frac{16 \pi \sigma^3 V_m^2}{3 \Delta\mu^2} , \qquad (8)$$

where $\Delta\mu$ is the thermodynamical driving force of the precipitation, the difference in the chemical potentials of the initial state and the precipitated state of the system glass/metal halide.

For pure metal halide precipitates (mole fraction ≈ 1) $\Delta\mu$ can be expressed by

$$\Delta\mu = RT \ln x_o + \varkappa^{-1} \sigma L^{1/3} V_m^{2/3} , \qquad (9)$$

using the model of regular solutions /13/ which was evidently shown to be valid for photochromic glasses /11/. R is the molar gas constant, x_o is the initial mole fraction of the metal halide in the glass, σ is the measured interfacial tension /1/, L is Avogadro's constant and $\varkappa$ is a semiempirical factor that varies in the range of 0,1 ... 0,45 for glasses /11,14,15/ (here $\varkappa = 1/3$).

Relating A_D to the viscous flow of the glass melt, J(nuclei $\cdot$ $cm^{-3} s^{-1}$) can be expressed in terms of the glass viscosity η

$$J = K'/\eta \exp(-A_K/kT) \quad , \qquad (10)$$

where the constant K' is equal to 10^{27} ... 10^{31} $cm^{-3}s^{-2}Pa^{-1}$ for sodium silicate glasses /15/. The viscosity η is equal to 10^{12} Pa·s for the temperatures near T_g used here. Therefore, the nucleation rates can be estimated considering the calculated values of A_K according to (8).

glass	$x_o\ 10^3$	$\frac{\mu}{10^3 Nm/mol}$	$\frac{J}{\text{nuclei } cm^{-3}\ s^{-1}}$
I	1,78	15,67	10^{-21} ... 10^{-17}
II	2,38	8,16	10^{-65} ... 10^{-61}
III	1,47	4,43	10^{-99}
IV	3,27	18,02	10^{-10} ... 10^{-6}

If we compare these results with those which are given in /11/ for AgCl in sodium borate glasses ($x_o = 4{,}5\ 10^{-2}$; $\Delta\mu = 7{,}2 \cdot 10^{-3}$ Nm/mol and consequently $J = 10^{10}$ ... $10^{14} cm^{-3}s^{-1}$, particle densities of 10^{15} obtained by homogeneous nucleation) a heterogeneous nucleation mechanism has to be concluded for our glasses, because the observed particle densities of 10^{14} ... 10^{16} cm^{-3} could not be formed by homogeneous nucleation within the available times of the heat treatment. Therefore, in order to obtain glasses of the investigated type with good photochromic properties, effective nucleating agents must be contained in the batch. This can be realized by small additions of ZrO_2 or/ and TiO_2 which are known to fulfil the requirements mentioned /17/.

References

1. Lembke, U.: Thesis, Wilhelm-Pieck-Universität Rostock, 1986
2. Schmidt, P.W.: Integral transform techniques for determining the particle-dimension distribution from the scattering data from systems of non-identical particles, Summer School "Diffraction Studies on Non-Crystalline Substances", Pecs, Hungary 1978
3. Gerber, T.: Thesis, Wilhelm-Pieck-Universität Rostock, 1983

4. Walter, G.; Kranold, R.; Gerber, T.; Baldrian, J.; Steinhart, M.: J.Appl.Cryst. 18 (1985) 205
5. Turnbull, D.: Acta Met. 1 (1953) 684
6. Ham, F.S.: J.Phys.Chem.Solids 6 (1958) 335
7. Lifshitz, I.M.; Slyozov, V.V.: J.Phys.Chem.Solids 19 (1961) 35
8. Wagner, C.: Z.Elektrochemie 65 (7/8) (1961) 581
9. Gmelins Handbuch der anorganischen Chemie, Silber, Syst.-Nr. 61 Teil B_1, 8. Auflage, Verlag Chemie, Weinheim 1971
10. Gutzow, I.; Schmelzer, J.; Pascova, R.; Popow, B.: Rostock. Phys.Manuskr. (1985), Heft 8, 22 - 30
11. Pascova, R.; Gutzow, I.: Glastechn.Ber. 56 (1983) 324 - 330
12. Volmer, M.: "Kinetik der Phasenbildung", Steinkopff, Dresden 1939
13. Becker, R.: Ann.Phys. 32 (1938) 128 - 140
14. Matusita, K.; Tashiro, M.: J.Non-Cryst.Solids 11 (1973) 471 - 483
15. Klein, L.C.; Handwerker, C.A.; Uhlmann, D.R.: J.Crystal Growth 42 (1977) 47 - 51
16. Hammel, J.J.: J.Chem.Phys. 46 (1967) 2234 - 2244
17. McMillan, P.W.: "Glass-Ceramics", Academic Press 1979

Authors:

Dr.rer.nat. Ulrich Lembke
Dr.rer.nat. Wolfhart Göcke
Prof.Dr. Winfried Blau
Wilhelm-Pieck-Universität Rostock
Sektion Physik
Universitätsplatz 3
Rostock
DDR - 2500

Rostocker Physikalische Manuskripte, Heft 12 (1988)

Armin Hoell; Rainer Kranold

Miscibility Gap Calculation for Nucleation Rate Determination in Soda-Line-Silica Glasses

1. Introduction

Liquid-liquid immiscibility is a widespread phenomenon in glass-forming systems /1/ and miscibility gaps, both stable and metastable, are known in many technologically important glass systems. Inside the gap phase separation can take place by nucleation and growth or by spinodal decomposition, depending whether the system is in the metastable or in the unstable part of the miscibility gap (see Fig. 1).

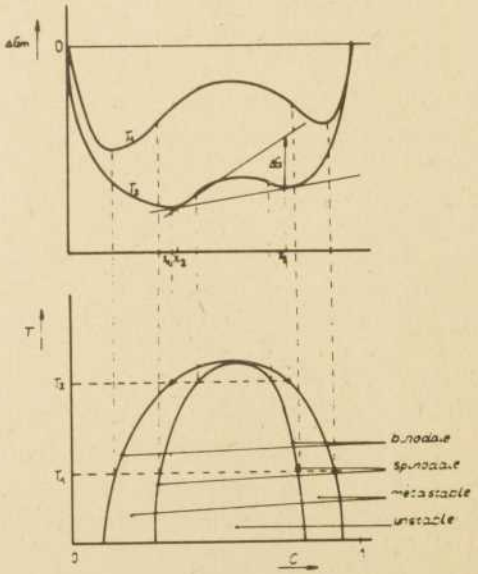

Fig. 1: Miscibility gap and free enthalpy of mixing for a binary system

We are dealt with the liquid-liquid phase separation in soda-line-silica glasses to improve the understanding of nucleation mechanisms in vitreous materials. This glass system is well

suitable, because many physical properties are known and it is possible to study liquid-liquid immiscibility without crystallization effects.

The soda-line-silica glass shows immiscibility in a silica-rich droplet phase and a matrix phase with reference to the SiO_2, that means the ratio of Na_2O to CaO is in matrix and droplet phase the same. Therefore, this system can be described as an pseudobinary one, signed by:

$$(1-x)SiO_2;\ x[y\,CaO + (1-y)\,Na_2O] \qquad \begin{matrix} 0 \leq x \leq 1 \\ 0 \leq y \leq 1 \\ y = \text{const} \end{matrix} \qquad (1)$$

where x, y are molar fractions.

The nucleation behaviour was examined by some authors /2,3, 4/. Hammel /4/ studied the immiscibility in a 13 Na_2O, 11 CaO, 76 SiO_2 (mol%) glass. He calculated the steady state nucleation rate for homogeneous nucleation, by using the appropriate energy difference, determined from the experimental miscibility gap /3/ and compared the calculated nucleation rate with the nucleation rate obtained by electron microscopic investigations.

The present paper discuss a possibility for the prediction of the immiscibility done in a ternary system using the known gaps of the binary subsystems. So it will be possible to calculate the miscibility gap, the corresponding driving force and the nucleation rate for any composition.

It was shown that the classical theory of nucleation in the Zeldovich-Frenkel formulation is a valuable tool in describing the nucleation behaviour /5/. In the first approximation it yields for the nucleation rate

$$I(t) = I_o \exp(-\tau/t) \qquad (2)$$

where I(t) - momentany rate of formation of critical nuclei, I_o - stationary rate of formation of critical nuclei, τ - induction time.

The expression for the stationary rate reads:

$$I_0 = \text{const} * \exp(-(W_k+W_a)/k_BT) \qquad (3)$$

where W_k - work of formation of critical nuclei, W_a - activation energy for the transport.

The change of the thermodynamic potential W_k due to the formation of a critical cluster can be written as consisting of three parts, one bulk term, one surface term and one term due to the elastic or viscoelastic deformation. In the case of spherical nuclei by neglecting the deformation term it holds:

$$W_k = \frac{16}{3} \pi \frac{\sigma^3 V_m^2}{\Delta G^2} \qquad (4)$$

where σ - interfacial tension, ΔG - thermodynamic driving force, V_m - molar volume of the glass.
In the following a method will be described to calculate suitable values of ΔG from the miscibility gap.

2. Calculation of the thermodynamic driving force

Figure 1 shows schematic the free enthalpy of mixing ΔG_m and the corresponding miscibility gap. x_1 and x_2 are the concentrations of matrix and nuclei in the equilibrium state. The expression for ΔG, the free enthalpy of mixing driving phase separation reads (Fig. 1):

$$\Delta G = \Delta G_m(x_2) - \Delta G_m(x_1) + (x_3 - x_2) \left(\frac{d\Delta G_m}{dx_2}\right) - \\ - (x_3 - x_2) \left(\frac{d\Delta G_m}{dx_1}\right) . \qquad (5)$$

A mathematical model of ΔG_m to calculate values of ΔG has to fit the measured immiscibility boundary. Several models were developed /6-8/.

For the present case of the soda-line-silica system Hammel /4/ compared the Lumsden model /6/ with the model developed by Von der Toom and Tiedema /7/. He found that the latter is extrem sensitive to small shifts in position of the immiscibility boundaries. Similar conclusions were drawn in /9/. According /4/ the Lumsden model /6/ yields good results. In that model is

$$\Delta G_m = x(1-x)\, f(x,T) + RT\,[(1-x)\ln(1-x) + x \ln x] , \qquad (6)$$

where

$$f(x,T) = \frac{c_1(T)}{(1-x)+r^2x} + \frac{c_2(T)}{(1-x)+r^5x} - (1-x)x\left\{\frac{c_1^2(T)}{ZRT[(1-x)+r^{8/3}x]^3}\right\}.$$

The model parameters c_1 and c_2 are linear functions of temperature T and must be determined by using the miscibility gap data. The Lumsden model is a special correction of the subregular solution model because it takes into account: (1) r, the ratio of radii of the components; (2) the average coordination number Z, and (3) the influence of the nonadjacent components.

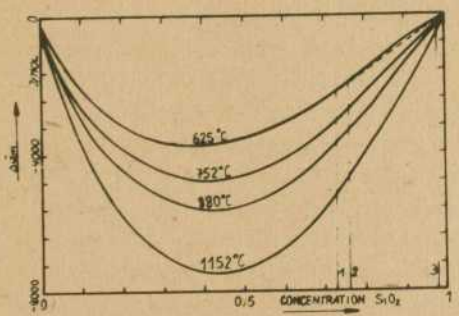

Fig. 2: Free enthalpy of mixing curves for the 13 $Na_2O \cdot 11\ CaO \cdot 76\ SiO_2$ (mol%) system for different temperatures T. The critical temperature is T_c=1152°C.

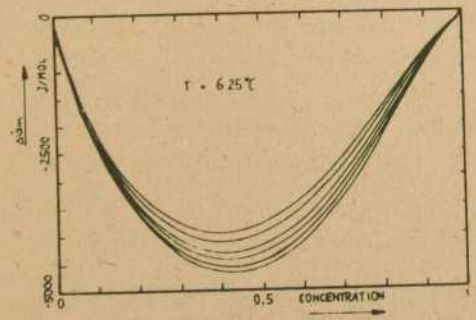

Fig. 3: Variation of the free enthalpy of mixing curves for the same system used in Fig. 2 obtained by slight variation of the immiscibility boundary. The curves from the upper to the lower correspond to curve numbers one to six in Table 1.

The free enthalpy of mixing ΔG_m calculated according to the Lumsden model are shown in Fig. 2 and 3. Figure 2 shows the variation of ΔG_m in dependence of temperature. For $T < T_c$ ΔG_m has two stable concentrations (compare the curve for 625°C), but for $T > T_c$ the solution is homogen. With (6) and (5) the driving

force ΔG for phase separations can be calculated. Substituting ΔG in (4), with (3) and (2), the nucleation rate can be obtained.

Table 1

Curve	T_1/K	x_{11}	x_{12}	T_2/K	x_{21}	x_{22}
1	1025	0.765	0,985	1153	0,8	0,98
2	1025	0,765	0,985	1153	0,803	0,977
3	1025,15	0,766	0,986	1153,15	0,803	0,977
4	1025	0,765	0,985	1425	0,904	0,904
5	1025	0,765	0,986	1425	0,904	0,904
6	1025	0,766	0,986	1425	0,9	0,9

To proof the sensibility of the Lumsden model to small shifts in positions of the immiscibility boundaries some calculations were made using the values given in Table 1. The results are shown in Fig. 3. Curve 1 is the same as used in /4/. It can be seen from Fig. 3 that slight variations of immiscibility data effect a drastic shift of the ΔG_m values. Taking into account the limited accuracy of experimental immiscibility data it must be stated that the values of the free enthalpy of mixing calculated using the Lumsden model must be called in question in some cases.

3. The calculation of the miscibility dome for a ternary system using the pseudobinary approximation

Hammel /4/ calculated the free enthalpy of mixing by utilization of the miscibility gap, which he measured for the ratio of Na_2O/CaO of 13/11. However, it would be advantageous to have a possibility which allowed to calculate the miscibility dome of the ternary system using the known miscibility gaps of the binary subsystems.

Kawamoto /10/ showed, that the immiscibility boundaries of some binary alkali or alkaline earth silicate systems can be superposed by normalizing immiscibility temperature T_m and composition c to a so called master curve. In Fig. 4 the relative temperature T_m/T_c is shown in dependence of the relative concentration c/c_m [$c/c_m = 1$ for $T_m/T_c = 0.8$]. Hereafter c_m at T_m/T_c = 0,8 is called c_m for simplicity.

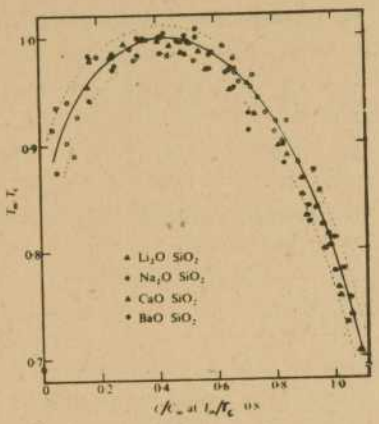

Fig. 4: Normalized immiscibility boundaries of some binary silicate systems and the master curve of immiscibility boundary (solid line) /10/.

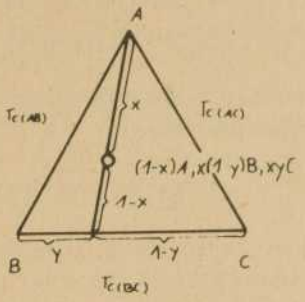

Fig. 5: Composition diagram for the ternary system A-B-C.

Furthermore, in /10/ it was predicted that any pseudobinary system chosen along a tie line in ternary silicate systems (Fig. 5) should have an immiscibility boundary with the same shape as that of the binary systems. Such behaviour must be expected if the model of regular mixing is applicable for the binary as well as the pseudobinary system. In this case the critical temperature T_c of the pseudobinary system can be calculated, using the critical temperatures of the binary subsystems by the equation (7),

$$T_c = y\, T_{c(AC)} + (1-y)\, T_{c(AB)} - y(1-y)\, T_{c(BC)} \cdot \qquad (7)$$

Furthermore, the expression for calculating c_m reads:

$$c_m = y\, c_{m(AC)} + (1-y)\, c_{m(AB)} \cdot \qquad (8)$$

Then, the miscibility gap of the pseudobinary system can be obtained using the molar curve and the T_c, c_m values calculated from (7) and (8), respectively.

In most cases values of $T_{c(BC)}$ in (7) are not available. However, suitable values of the parameters $T_{c(BC)}$, which not necessary must have a physical meaning, can be calculated if the tem-

perature T_m^* of the miscibility gap of a glass with composition

(1-x) A•x (1-y) B•xy C

is determined experimentally. From (8) for c/c_m follows:

$$\frac{c}{c_m} = \frac{x}{y\, c_{m(AC)} + (1-y) c_{m(AB)}} \quad . \tag{9}$$

Therefore, using the master curve the unknown value $T_{c(BC)}$ can be computed, where

$$\frac{T_m}{T_c} = \frac{T_m^*}{y\, T_{(AB)} + (1-y) T_{c(AC)} - y(1-y) T_{c(BC)}} \quad . \tag{10}$$

Now, it is possible to calculate immiscibility isotherms for any temperatures. For that purpose it is only necessary to vary the molar fraction y in (10) and by using the master curve to calculate the corresponding molar fractions x from (9). An assembly of computed immiscibility isotherms for the soda-line-silica system is shown in Fig. 6. The experimental value T_m^* used for the calculation was taken from /3/.

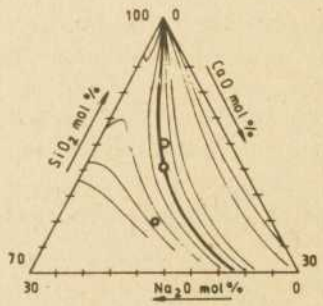

Fig. 6: Estimated immiscibility isotherms of the Na_2O-CaO-SiO_2 system. The circles indicate T_m^* values (from the upper to the lower: T_m=1000°C,980°C /3/ and 704°C /4/). The temperature T_m^*=980°C was used for the calculations. The curves yield for 600,700,800,900,980,1000, 1100,1200,1600 and 1800 (all in °C), from the left to the right hand side.

The calculated isotherms are in good agreement with the T_m^* values of Table 1 in /3/ and the value $T_m^* = 704^oC$ which was used by Hammel for his calculations. (Note, that the temperature $T_m^* = 1140^oC$ (in Table 1 of /3/ must be corrected to $T_m^* = 1000^oC$.) Moreover, the immiscibility isotherms, calculated using other experimental results from /3/, are in accordance with Fig. 6. Slight deviations can be observed only in the region of the phase diagram poor on CaO where the immiscibility isotherms have a saddle-point. It must be pointed out, that the saddle-point is

a relative flat one. Therefore, the insecurities of the master curve and the T_m^* values take effect especially in this region of the phase diagram.

In contrast to Fig. 6 the in /10/ calculated phase diagram of the soda-line-silica glass has not a saddle-point. This may be result from the incorrect choise of the value T_m^* = 1140°C for the composition 7,5 Na_2O-7,5 CaO-85 SiO_2. Despite of the fact, that up to now the existence of a saddle-point in the immiscibility isotherms of the soda-line-silica system was not proofed experimentally, there are some evidence that our calculations are essentially correct. Calculations of the immiscibility isotherms magnesia-alumina-silica system carried out recently reveal that a well pronounced saddle-point occurs, the existence of which was confirmed experimentally /11/.

4. Conclusions

To summarize the results described above it can be concluded that the values of the free enthalpy of mixing computed by the aid of the Lumsden must be handled with care. Maybe that other models, e.g. those described in /8/, would lead to more stable solutions. The influence of various ΔG_m values obtained by different models on the calculated nucleation rate has to be examined. Note that an exact determination of the interface tension σ is an unsolved problem.

The temperature of the immiscibility boundary is extreme sensitive to small shifts in the composition, particular near the edge of the miscibility gap where the nucleation theory should apply. Therefore, a method to calculate exact values of the temperature for any composition would be very useful. It seems to us that the discussed method of Kawamoto /10/ can be used successful for this purpose. However, it should be noted that this model can only applied inside the limits of immiscibility which must be proofed experimentally for every system.

References

1. Vogel, W.: Glaschemie, VEB Deutscher Verlag für Grundstoffindustrie, Leipzig 1979
2. Straad, Z.; Douglas, R.W.: Physics and Chemistry of Glasses 14 (1973) 33
3. Burnett, D.G.; Douglas, R.W.: Physics and Chemistry of Glasses 11 (1970) 125
4. Hammel, J.J.: The Journal of Chemical Physics 46 (1967) 2234
5. Gutzow, I.; Toschev, S.: in "Advances in Nucleation and Crystallization in Glasses", Eds.: Hench, L.L.; Freiman, S.W., Ohio 1971
6. Lumsden, J.: Thermodynamics of Alloys, London 1952
7. Von der Toom, L.J.; Tiedema, T.J.: Acta Metallurgica 8 (1960) 711
8. Lukas, H.L.; Weiss, J.; Henig, E.Th.: Calphad 6 (1982) 229
9. De Fontaine, D.; Hilliard, J.E.: Acta Metallurgica 13 (1965) 1019
10. Kawamoto, Y.; Tomozawa, M.: Physics and Chemistry of Glasses 22 (1981) 11
11. Galachow, F.Ja.: Awerjanow, W.I.; Wawilonowa, W.T.; Areschew, M.P.: Fisika i chimija stekla 2 (1976) 412

Authors:

Dipl.-Phys. Armin Hoell and Dr. rer. nat. Rainer Kranold
Wilhelm-Pieck-Universität Rostock
Sektion Physik
Universitätsplatz 3
Rostock
DDR - 2500

Rostocker Physikalische Manuskripte, Heft 12 (1988)

Manfred Dubiel, Doris Ehrt

Investigations of the Crystallization on Fluoroaluminate Glasses Using Nuclear Magnetic Resonance

In the last few years the applications of fluoroaluminate glasses are increased considerably because of their favourable properties as for instance the abnormal partial dispersion which makes the glasses suitable to correct the chromatic aberration in dense systems /1,2/. A special problem for manufacturing of these glasses is the strong crystallization tendency. The crystallization products only were detected and identified up to now with X-ray diffraction, polarization microscopy, wideline and high-resolution nuclear magnetic resonance /3-5/. However the exact knowledge of the nucleation process up to the completely crystallized sample is necessary to prevent the crystallization. For it exist no results.

One method for structure investigations is the nuclear magnetic resonance (nmr). Using wideline nmr it could be shown the similarity of the short range order in the amorphous and crystalline state /5/. That means that this method, which is only sensitive to the nearest neighbourhood, is not suitable to observe the crystallization kinetics. High-resolution experiments showed a line narrowing due to the crystallization /4/. Essential higher effects were detected measuring the spin-lattice relaxation time T_1 by the transition in the crystalline state on different systems /6-9/. Therefore it was measured the spin-lattice relaxation time T_1 of the nuclei ^{19}F in the fluoroaluminate glasses and the corresponding recrystallization products of the composition $M(PO_3)_2$ - CaF_2 - AlF_3 (M: Ba, Sr) with a CaF_2/AlF_3 ratio from 1,33 to 1,5 (see Fig. 1). In these cases the T_1 was changed by a factor in the range from 2 to 10. It is necessary to describe the process which is responsible for the spin-lattice relaxation for a detailed interpretation of these results.

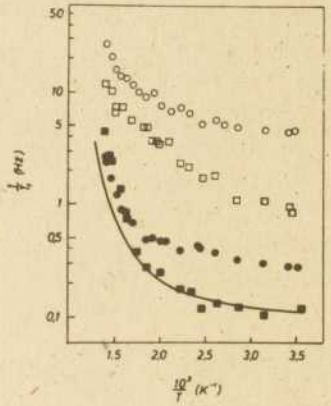

Fig. 1:
Comparison of the relaxation rates in the amorphous (open symbols) and polycrystalline (full symbols) state of the glasses 5 mol% $Ba(PO_3)_2$ - 54 mol% CaF - 41 mol% AlF_3 (o) and 5 mol% $Sr(PO_3)_2$ - 54 mol% CaF_2 - 41 mol% AlF_3 (□). Moreover the relaxation rate of the polycrystalline sample with the composition 60 mol% CaF_2 - 40 mol% AlF_3 is shown (full line)

It is known from analyzing the fluoroaluminate glasses that in all samples a certain content of paramagnetic impurities is given (ca. 20 ... 30 ppm), mainly as Fe^{3+}, which is caused by the starting materials and the preparation technique. Because of the strong influence of these ions on the relaxation process it is necessary to find the relation between their concentration and the T_1. To that end it was measured T_1 in dependence on the nmr-frequency and the temperature by a series of samples additionally doped with Fe_2O_3. From that it could be shown that the relaxation rate $1/T_1$ consists of two parts:

$$1/T_1 = 1/T_{1_{para}} + 1/T_{1_{pure}} \qquad (1)$$

The first contribution to the total relaxation rate $1/T_1$ comes from the Fe^{3+} incorporation. It can be described from 300 up to 450 K by the diffusion limited relaxation and from 450 K up to the glass transformation temperature by the atomic diffusion of the paramagnetic impurities /10,11/. The second part is induced by a specific relaxation process of glasses.

In the following the glasses were investigated which were not additionally doped. It was considered only the measured value at room temperature $T_{1_{rt}}$ for the further calculations. The T_1 of the glass $T_{1_{rt,glass}}$ and of the completely crystallized sample

$T_{1_{rt,cryst}}$ were chosen as reference points. In order to interprete the experimental results one can assume that the sample is divided into many regions ΔV of the same volume. Supposing that n_1 regions show an amorphous and n_2 regions crystalline relaxation behaviour, respectively, the reciprocal relaxation time of the whole sample is given by

$$\frac{1}{T_{1_{rt}}} = \frac{1}{n_1+n_2}\left\{n_1 \frac{1}{T_{1_{rt,glass}}} + n_2 \frac{1}{T_{1_{rt,cryst}}}\right\} \qquad (2)$$

Commonly the restriction of motion processes by the glass-crystal transition leads to a prolongation of $T_{1_{rt}}$ and with that to a reduction of the rate $T_{1_{rt}}^{-1}$. Therefore it is possible to calculate the crystallized part of the volume x by the time dependent relaxation rate $T_{1_{rt}}^{-1}$ during the isothermal crystallization process as follows

$$x(t) = \frac{n_2}{n_1+n_2} = \frac{T_{1_{rt}}^{-1}(t) - T_{1_{rt,glass}}^{-1}}{T_{1_{rt,cryst}}^{-1} - T_{1_{rt,glass}}^{-1}} \qquad (3)$$

The isothermal crystallization of several samples was investigated in the neighbourhood of the maximum of the crystallization. The samples were quenched to room temperature in fixed temporal intervals in order to measure T_1. Besides of them the degree of crystallization was checked by X-ray diffraction. To calculate the time dependent crystallized part of the volume the following formula was used /12,13/

$$x = 1 - \exp\left[-(Kt)^n\right] \qquad (4)$$

n is characterized by the crystalline growth mechanism and K represents the effective rate of reaction containing the activation energy of crystallization. It could be estimated a value of $n \approx 1$ for the sample of the composition 5 mol% $Sr(PO_3)_2$ - 54 mol% CaF_2 - 41 mol% AlF_3 between 850 and 903 K (see Fig. 2). X-ray experiments have identified the main crystalline phase to be Ca_2AlF_7. The investigations by means of polarization microscopy showed a two dimensional growth of the crystals in the volume.

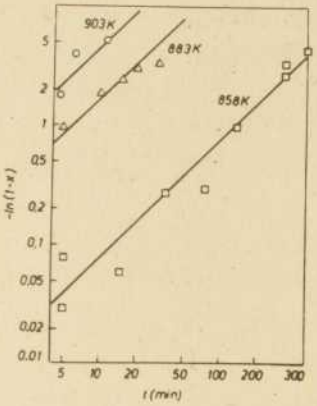

Fig. 2:
Representation of the crystallized volume fraction x in dependence on the time t (assuming $n \approx 1$)

Excluding a surface crystallization which was not observed one can conclude of a process with heterogeneous nucleation and a diffusion limited growth of the crystals /14,15/.

The summary of these results leads to the conclusion that in special cases also with the nuclear magnetic resonance spectroscopy measuring the spin-lattice relaxation time T_1 it is possible to find informations on the crystallization of glasses. The advantages of this method are the sensitivity of T_1 and the possibility to observe processes with a high reaction rate.

References

1. Ehrt, D.; Vogel, W.: Feingerätetechnik 31 (1982) 147
2. Ehrt, D.; Atzrodt, R.; Vogel, W.: Wiss.Zeitschr.FSU Jena, Mathem.-Naturwiss.R. 32, 2/3 (1983) 509
3. Ehrt, D.: Thesis, FSU Jena 1984
4. Krauss, M.: Thesis, FSU Jena 1984
5. Dubiel, M.; Bärenwald, U.; Ehrt, D.; Krauss, M.: Rostock. Physikal.Manuskripte 7 (1985) 86
6. Haupt, J.: Proc. XVIthe Colloque Ampére Bukarest 1970, 630
7. Krämer, F.; Müller-Warmuth, W.; Scheerer, J.; Dutz, H.: Z.Naturf. 28a (1973) 1338
8. Rubinstein, M.; Resing, H.A.; Reinecke, T.L.; Ngai, K.L.: Phys.Rev.Lett. 34 (1975) 1444

9. Rubinstein, M.; Resing, H.A.: Phys.Rev. B14 (1976) 959
10. Bolembergen, N.: Physica 15 (1949) 386
11. Shen, L.: Phys.Rev. 172 (1968) 259
12. Johnson, W.A.; Mehl, K.F.: Trans.Am.Inst.Mining Met.Engns. 135 (1981) 315
13. Avrami, M.: J.Chem.Phys. 7 (1939) 1103; 8 (1940) 212; 9 (1941) 177
14. Mandelkorn, L.: in: Doremus, R.H.; Roberts, B.W.; Turnbull, D. "Growth and Perfection of Crystals", Wiley & Sons Inc., New York; Chapman & Hall, London 1958
15. Mac Farlane, D.R.; Fragoulis, M.: Phys.&Chem.of Glasses 27, 6 (1986) 228

Authors:

Dr. Manfred Dubiel
Martin- Luther-Universität Halle-Wittenberg
Sektion Physik
Halle
DDR - 4020

Dr. Doris Ehrt
Friedrich-Schiller-Universität Jena
Sektion Chemie
Jena
DDR - 6900

Rostocker Physikalische Manuskripte, Heft 12 (1988)

Rainer Kranold; Wolfgang Schiller

Nonuniformity of Cation Distribution and Crystallization Behaviour of Single Phase Glasses in the $BaO-SiO_2$ System

1. Introduction

It is well known that many glasses are chemical and structural nonuniformly since liquid-liquid phase separation has been discovered 30 years ago. Moreover, evidence has been accumulated that also the structure of single phase glasses (one component glasses or glasses outside the miscibility gap of the phase diagram) often is not so uniform as have been assumed over a long interval of time /1/. Unfortunately, there are only few investigation methods for recognizing such kind of nonuniformity. A special problem which can be successfully studied by X-ray diffraction techniques is the distribution of network modifier cations inside of the glass network /2,3/. Roy /1/ predicted that if there is compositional and/or structural nonuniformity, this will result in the crystallization of unexpected phases and almost certainly a two-step crystallization. Such two-step crystallization is well known /4-7/ from glasses in the single phase part of the phase diagram of the $BaO-SiO_2$ system shown in Fig. 1. The schematic representation of the DTA diagram of a glass with composition 3 $BaO \cdot 5\ SiO_2$ is given in Fig. 2. In a previous work /7/ it was shown that during the first step of crystallization starting at temperature T_1 in Fig. 2 the crystallization of a metastable crystal phase, which has a higher content than the glass composition, takes place followed immediately by the crystallization of another metastable crystal phase, the boria content of which is lower than that of the glass. During the second step starting at T_2 the primary crystal phases and the residuum glass phase react to form the thermodynamic stable crystal phase having the same stoichiometric composition as the glass.

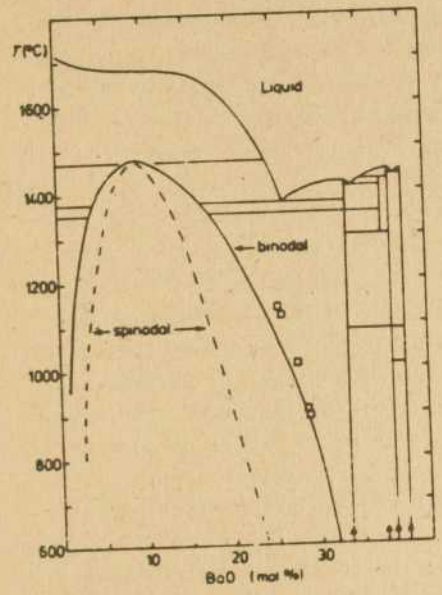

Fig. 1:
Phase diagram of a section of the $BaO-SiO_2$ system (from /8/). The arrows indicate the compositions of the crystal phases $BaO \cdot 2\,SiO_2$, $3\,BaO \cdot 5\,SiO_2$, $5\,BaO \cdot 8\,SiO_2$, and $2\,BaO \cdot 3\,SiO_2$.

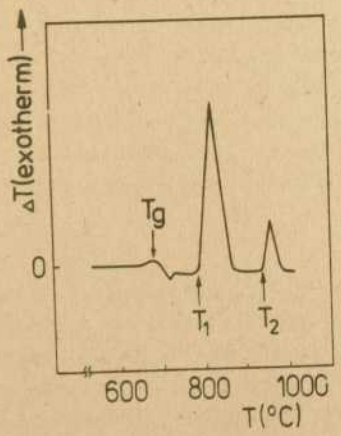

Fig. 2:
Schematic representation of the DTA curve of a glass with composition $3\,BaO \cdot 5\,SiO_2$ (after /6,7/)

The aim of the present paper is to investigate by X-ray diffraction whether there are regions with different boria content in the non-crystallized origin glass or not. The $BaO-SiO_2$ system

has several ideal features for investigations of this kind. It exhibits internal (volume) crystal nucleation without deliberate addition of nucleation catalysts, and the large scattering power of Ba causes that the Ba-Ba distances have large influence on the X-ray pattern.

2. Sample Preparation

The starting glass with 37 mol% BaO, i.e. close to the 3 BaO·5 SiO_2 composition, was prepared from high purity commercial sand and reagent grade $BaCO_3$. The components were fused in an inductive heated Pt-10%Rh crucible at 1570°C for 7 h. During melting the glass was stirred. Then, the glass was fritted, finely crushed and remelted twice at 1550°C for 4 h. This melt was cast on a mould, than transferred to an annealing furnace maintained at 500°C and furnace cooled. Finally, in order to avoid stresses, the glass was reheated and after a heat-treatment at 600°C for 2 h cooled down with a cooling rate of about 1 $Kmin^{-1}$. Pieces of the glass were isochronal heat-treated at various temperatures for 2 h from 650°C to 750°C (the glass-transition temperature is T_g = 680°C). Subsequently the specimens were visibly clear of good optical quality.

The BaO, SiO_2 contents of the glass determined by X-ray fluorescence analysis as well as by wet chemical analysis were obtained to be very close to the nominal ones. The main impurity was SrO (0.7 wt %) introduced by the $BaCO_5$ starting material. The total content of the other impurities was found to be lower than 0.05 wt %.

3. X-Ray Diffraction Procedures

Thin polished samples with dimensions of approximately 20 x 10 x 0.09 mm^2 were used for the X-ray studies. The diffraction patterns were obtained /9/ using a non-focusing diffractometer with a flat graphite crystal monochromator in the primary beam. A Rigaku Denki rotating-anode generator with an Ag target was operated at 45 kV and 200 mA. Counts were made in steps of 0.3° in the interval of the scattering angle θ from 2° to 122°. Special efforts were made to eliminate the influence of the fluorescence

radiation, which was produced by the Sr content of the glass, by combining the measurements carried out with and without a Zn-filter in the diffracted beam.

The measured intensities were corrected for background, absorption, polarization, and complex scattering and then converted to electron units per unit of composition (eu/uc). Subsequently the normalized intensity I(s) was Fourier transformed to give the pair function distribution (PFD) introduced by Warren /10/, where $s = 4\pi/\lambda \sin(\vartheta/2)$ and λ is the X-ray wavelength. The PFD is defined by equation (1)

$$\sum_{uc} \sum_{i} \frac{N_{ij}}{r_{ij}} P_{ij}(r) = 2\pi^2 r \varrho_e \sum_{uc} z_j + \int_0^{s_{max}} s\, i(s) e^{-\alpha^2 s^2} \sin(sr)\, ds, \qquad (1)$$

with

$$i(s) = [I(s) - \sum_{uc} f_j^2]/f_e^2(s) \quad , \qquad (2)$$

where f_j is the atomic scattering factor for atom "j", and f_e is the average scattering factor of an electron. The expression $\exp(-\alpha^2 s^2)$ is a convergence factor, r is a radial distance, ϱ_e is the average electron density, s_{max} is the cutoff-value of s, z_j is the number of electrons in atom "j", N_{ij} is the number of neighbours in the i-th shell about atom "j", r_{ij} is the distance from an atom "j" to an atom in the i-th shell, and $P_{ij}(r)$ is the pair function given by

$$P_{ij}(r) = \int_0^{s_{max}} \frac{f_i f_j}{f_e^2(s)} e^{-\alpha^2 s^2} \sin(sr_{ij}) \sin(sr)\, ds \, . \qquad (3)$$

The right-hand side of (1) is the experimental pair function distribution $(PFD)_{exp}$. An important advantage of the PFD method is given by the possibility to compare $(PFD)_{exp}$ with the calculated pair function distribution $(PFD)_{calc}$ of suitable structural models using the left-hand side of (1). Full details of measurements and data analysis are given in /11/.

The X-ray scattering in the small-angle range was measured with a commercial Kratky camera in the interval of s between 0.2 nm^{-1} and 1 nm^{-1} using Mo radiation. A Nb filter was used in the primary beam, and the scattered $K\alpha$ radiation was detected

with a scintillation counter in conjunction with a pulse-height analyzer. To convert the measured intensities in electron units a calibrated Lupolen standard sample was used. The corrected intensity, which is nearly angle-independent at small s-values, was extrapolated to the zero-angle using a least-squares method. The zero-angle intensity $\tilde{I}(0)_{Fl}$ represents a measure for the fluctuations of the electron density in the glass. Full details of the accurate determination of the $\tilde{I}(0)_{Fl}$ parameter are given elsewhere /12/.

Using the Bhahia-Thornton formalism /13/, for a binary system in the liquid or frozen in state containing components A and B with atomic scattering amplitudes b_A and b_B, the intensity $I(0)_{Fl}$ expressed in electron units per atom can be written

$$I(0)_{Fl} = \langle b \rangle^2 S_{NN}(0) + [(b_B - b_A) - \delta \langle b \rangle]^2 S_{CC}(0) \quad . \qquad (4)$$

The first term results from fluctuations of particle density and the second term from concentration fluctuations. The parameter δ describes the differences in size of the species A,B. For a structure frozen in a fictive temperature T_f both density and concentration fluctuations can be expressed by the thermodynamic relationships (5) and (6)

$$S_{NN}(0) = k\, T_f\, \varkappa(T_f)/V_a \qquad (5)$$

$$S_{CC}(0) = k\, T_f\, (\partial^2 G/\partial c^2)^{-1} \quad , \qquad (6)$$

where G is the free enthalpy of mixing, c is the concentration of component B, k is the Boltzmann constant, V_a is the average atomic volume, and $\varkappa(T_f)$ is the isothermal compressibility at T_f. Mostly, T_f is replaced by the glass-transition temperature T_g.

4. Results and Discussion

The scattering curve of the unheated glass (Fig. 3) shows a sharp pronounced main peak at $\vartheta = 10^0$ ($s = 19.5\ nm^{-1}$). Compared with the scattering curves of pure vitreous silica, where the main peaks have their position at about $s = 15\ nm^{-1}$, the 37 mol% BaO content leads to a considerable peak displacement to the direc-

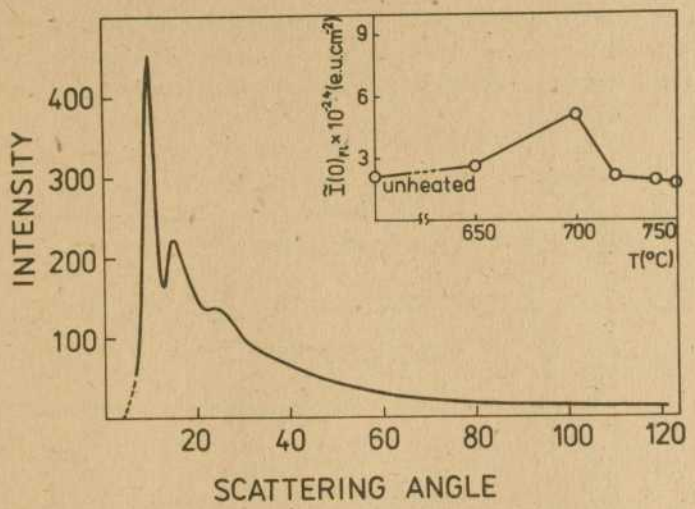

Fig. 3: Scattered intensity of the unheated 0.37 BaO·0.63 SiO_2 glass. The insert shows the $\bar{I}(0)_{FL}$ parameter in dependence on the temperature of heat-treatment.

tion of higher s-values. This is the characteristic feature observed for the scattering curves of binary silicate glasses /14/. There are no remarkable distinctions between the scattering curves of the unheated glass and the glass sample heat-treated at 750°C for 2 h. Particularly, crystalline reflections of no sort have been observed. However, replica electron micrographs of the heat-treated glass show individual spherulitical particles of 100 - 500 nm in size /7/. After a second heat-treatment at 800°C for 5 min, 5 BaO·8 SiO_2, which has a higher boria content than the average glass composition, was identified as first crystallization product by X-ray powder diffraction. Immediately after this process, crystallization of the high-temperature form of BaO·2 SiO_2, the boria content of which is less than that of the glass, has been observed.

Fig. 4(a) shows the pair function distribution $(PFD)_{exp}$ of the unheated glass (solid line) and that of the glass heat-treated at 750°C for 2 h (dotted line). There are hardly diffe-

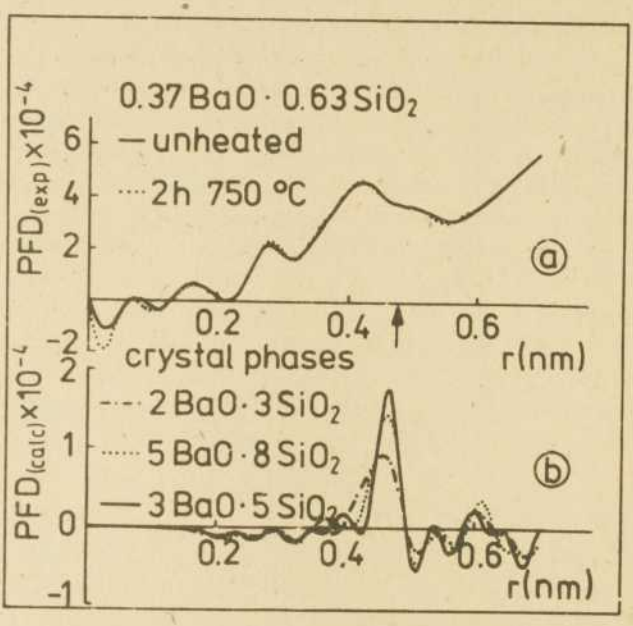

Fig. 4: Pair function distributions of the unheated and the heat-treated glass samples (a) and the PFDs calculated for different crystal phases (b)

rencies between the two curves, but the peaks in the latter are somewhat more pronounced. The pair function distributions $(PFD)_{calc}$ of the three boria-rich crystal phases of interest here calculated using the crystal structure data given in /15/ are shown in Fig. 4(b). By calculation of the separated pair functions for the crystal phases it can be easily shown that the main peaks in the $(PFD)_{calc}$ curves nearly r = 0.45 nm are caused by the Ba-Ba pairs /9/. Therefore, it can be assumed that the main peaks in the $(PFD)_{exp}$ curves likewise are mainly caused by the Ba-Ba distances in the glass network. From Fig. 4(a) it becomes evident that the Ba ions are not distributed uniformly throughout the glass but that their average distance, the magnitude of which is not changed by the heat-treatment, is considerable less than that for a uniform distribution indicated by

the arrow. Furthermore, comparing the Figs. 4(a) and (b), it can be concluded that the distances of the Ba ions in the glass seems to be smaller than those in the crystal phases. Note that the density of the glass (3.95 gcm^{-3}) is higher than that of the primary crystal phase 5 $BaO \cdot 8\ SiO_2$ /4/.

The PFD method is insensitive to local variations of the short-range order beyond the first few atom diameters. Therefore, it is not possible to make a decision whether the Ba ions in the glass are concentrated in "clusters" or "ion swarms" or, if there are discrete, molecule like, groups with small Ba-Ba distances distributed uniformly throughout the glass. The zero-angle intensity $\tilde{I}(0)_{F1}$, (4), which is sensitive to variations of the electron density fluctuations in the glass, may be used to decide this questions.

For the present case of the 0.37 $BaO \cdot 0.63\ SiO_2$ glass, the thermodynamic data needed for the exact evaluation of (4), (5), and (6) are not available. Therefore, it was renounced of a collimation correction procedure for the small-angle scattering curves and in the insert of Fig. 3 the "slit-smeared" $I(0)_{F1}$-values are shown. The diagram shows that starting from the unheated glass the values of the $\tilde{I}(0)_{F1}$ parameter increase with increasing temperature of heat-treatment up to a temperature of 700°C and after that decrease to a level less than for the origin glass. From (5) it is obvious that the observed drastic changes of the $I(0)_{F1}$-values cannot be caused by the particle density term of (4) because the fictive temperature T_f and/or the isothermal compressibility $\varkappa(T_f)$ cannot change to such high degree for this kind of heat-treatment. Therefore, it must be stated that the changes in the values of the $\tilde{I}(0)_{F1}$ at heat-treatments near T_g indicate the clustering of Ba ions. The drop up of $\tilde{I}(0)_{F1}$ observed for the glass specimens heat-treated at higher temperatures can be explained by the increasing degree of structural order in the separated glass regions which effects that the total amount of the electron density fluctuations decreases. For the specimens heat-treated at 740°C and 750°C, where electron micrographs show individual crystalline particles, the $\tilde{I}(0)_{F1}$ parameter takes values comparable to those ob-

tained for vitreous silica under the same experimental conditions /16/. It can be supposed that the most developed baria-rich clusters act as sites for the nucleation of the metastable primary crystal phase 5 BaO·8 SiO_2. In fact, the first observation of particles, larger than 30 nm in size and with a sharp interface boundary, was made by small-ange X-ray scattering in the sample heat-treated at 720°C for 2 h /9/, that means immediately after the $\tilde{I}(0)_{F1}$ parameter lead off to drop. Note that this kind of heat-treatment is designated in /5/ as the optimal one to form crystalline nuclei in glasses of the actual composition.

5. Summary

The Ba cations are not distributed uniformly in the 37 mol% BaO single phase BaO-SiO_2 glass but there are local separated regions which are baria-rich and other with a lower baria content. The consequence of this feature is that in the first step of crystallization of the glass metastable crystal phases with stoichiometric compositions 5 BaO·8 SiO_2 and BaO·2 SiO_2, respectively, are formed rather than the thermodynamically stable 3 BaO·5 SiO_2 phase.

References

1. Roy, R.: in: Advances in Nucleation and Crystallization in Glasses (ed. by L.L. Hench and S.W. Freiman), Special Publ. of the Amer.Ceram.Soc. No. 5, Ohio 1971, p. 51
2. Hilberg, M.E.; Peters, C.R.: Phys.Chem.Glasses 10 (1969) 46
3. Herms, G.; Göcke, W.: Wiss.Zeitschr.WPU Rostock 24 (1975) 567
4. Mac Dowell, J.F.: Proc.Brit.Ceram.Soc. 3 (1965) 229
5. Freiman, S.W.; Onada, Ju.G.Y.; Pincus, A.G.: J.Amer.Ceram. Soc. 55 (1972) 354
6. Oehlschlegel, G.: J.amer.Ceram.Soc. 58 (1975) 148
7. Schiller, W.; Kosche, J.; Schröter, Ch.; Wiegmann, J.: 2. Int.Otto-Schott-Kolloquium (Posterbeiträge), Wiss.Beiträge FSU Jena 1983, p. 93
8. Ramsden, A.H.; James, P.F.: J.Mater.Sci. 19 (1984) 1406

9. Kranold, R.; Steil, H.; Schiller, W.: XIX. Jahrestagung der VFK (Kurzreferate), Rostock 1985, p. 100
10. Warren, B.E.: X-Ray-Diffraction, Addison-Wesley Publ. Co., Massachusetts 1969
11. Steil, H.: Ph.D.thesis, Wilhelm-Pieck-Univ.Rostock, 1979
12. Göcke, W.; Enenkel, N.; Walter, G.; Kranold, R.: studia biophysica 97 (1983) 135
13. Bhatia, A.; Thornton, D.E.: Phys.Rev. B2 (1970) 3004
14. Wiegmann, J.
15. Hesse, K.-F.; Liebau, F.: Z.Kristalogr. 153 81980) 3
16. Enenkel, N.: Ph.D. thesis, Wilhelm-Pieck-Univ.Rostock, 1983

Authors:

Dr. Rainer Kranold
Wilhelm-Pieck-Universität Rostock
Sektion Physik
Universitätsplatz 3
Rostock
DDR - 2500

Dr. Wolfgang Schiller
Zentralinstitut für Anorganische Chemie
der AdW der DDR
Rudower Chaussee 5
Berlin
DDR - 1199

Rostocker Physikalische Manuskripte, Heft 12 (1988)

Frank Schweitzer

Thermodynamic Investigations of Nucleation in Binary Finite Systems

A thermodynamic analysis of a two-phase system may lead to a deeper insight into the conditions of a first order phase transition /1/. The knowledge of the exact thermodynamic potential of the system allows us to calculate the critical and stable cluster size for a phase transition /2/, furthermore, critical thermodynamic constraints for a nucleation process in an one-component finite system are determined /2,3/.

Former investigations gave a general thermodynamic analysis of a heterogeneous k-component system considering the change of the initial matrix phase by the formation of the new phase /2, 4,5/. These results have been applied mainly to nucleation and cluster growth in one-component systems /6/, but also the kinetics of condensation in binary vapours /7/, the decomposition of solid solutions /6/, and Ostwald ripening of bubbles in liquid-gas solutions /8/ have been discussed based on a thermodynamic approach.

This paper continues the thermodynamic analysis. As done before, we consider the limitation of the total particle number of the system, that means a matrix depletion caused by the formation of clusters of a new phase.

1. Thermodynamics of a heterogeneous binary system

For a homogeneous binary system the inner energy is usually given by:

$$U_{hom} = TS - pV + \mu_1 n_1 + \mu_2 n_2 \qquad (1.1)$$

In the heterogeneous state we have two phases α and β, which are divided by a boundary phase, indicated by the index o. The inner energy of the heterogeneous system is then given by /9/:

$$U_{het} = U_\alpha + U_\beta + U_o \tag{1.2}$$

with the contributions

$$U_\alpha = T_\alpha S_\alpha - p_\alpha V_\alpha + \mu_{1\alpha} n_{1\alpha} + \mu_{2\alpha} n_{2\alpha} \tag{1.3}$$

$$U_\beta = T_\beta S_\beta - p_\beta V_\beta + \mu_{1\beta} n_{1\beta} + \mu_{2\beta} n_{2\beta} \tag{1.4}$$

$$U_o = T_o S_o + \mu_{1o} n_{1o} + \mu_{2o} n_{2o} + \sigma A \tag{1.5}$$

The boundary phase is here assumed to be the Gibbsian surface of tension /9/, σ being the surface tension and A the surface area. n_{io} and S_o denote excess values caused by deviations from additivity in the heterogeneous state:

$$n_{io} = n_i - n_{i\alpha} - n_{i\beta} \qquad i = 1,2 \tag{1.6}$$

$$S_o = S - S_\alpha - S_\beta \tag{1.7}$$

Formally n_{io}, S_o can be interpreted as thermodynamic values of the surface. For the surface energy U_o (eq. 1.5) the Gibbs-Duhem relation is valid:

$$S_o dT_o + A d\sigma + n_{1o} d\mu_{1o} + n_{2o} d\mu_{2o} = 0 \tag{1.8}$$

For a former discussion of the surface part we use the condition of an internal equilibrium of both phases α and β /4,10/, that means an inner equilibrium and a quasi-stationary change of these states. Because a surface phase has no real autonomy in general/11/, we are allowed to replace the intensive variables of the surface by the corresponding values of one of the coexisting phases α or β . It seems to be reasonable that the phase with a larger density should determine the surface values T_o and μ_{io} /4/. We denote in the following the matrix phase by β and the evolving phase by α and assume further α to be the phase with a higher density (like in gas-liquid phase transitions).

Eq. (1.8) is then replaced by /4,12/:

$$-d\sigma = s_o dT_\alpha + \Gamma_{1o} d\mu_{1\alpha} + \Gamma_{2o} d\mu_2 \tag{1.9}$$

with Γ_{io} being the surface particle densities and s_o the surface entropy density:

$$\Gamma_{io} = \frac{n_{io}}{A} \quad , \quad i = 1,2 \qquad s_o = \frac{S_o}{A} \tag{1.10}$$

Considering a heterogeneous system established by a nucleation process eq. (1.9) means that the surface tension σ should be determined by the quantities describing the evolving phase α. In particular we find for the surface tension dependent on the temperature T_α and on the mole fraction x_α of the nucleus:

$$\frac{\partial \sigma}{\partial T_\alpha} = - s_o - \sum_{i=1}^{2} \Gamma_{io} \frac{\partial \mu_{i\alpha}}{\partial T_\alpha} \tag{1.11}$$

$$\frac{\partial \sigma}{\partial x_\alpha} = - \sum_{i=1}^{2} \Gamma_{io} \frac{\partial \mu_{i\alpha}}{\partial x_\alpha} \tag{1.12}$$

Consequently, the usual approximation $n_{io} \simeq 0$ results in a dependence of σ on the temperature only, but no longer on the molar fraction of the nucleus.

In the following we restrict ourselves to isothermal systems, that means $T_\alpha = T_\beta = T$, and fix the thermodynamic constraints as follows:

$$n = \text{const.}, \; V = \text{const.}, \; T = \text{const.} \tag{1.13}$$

Now the free energy $F = U - TS$ is the thermodynamic potential to describe the heterogeneous system. We calculate the change of the free energy for a transition from the initial homogeneous to the final heterogeneous system:

$$\Delta F = F_{net} - F_{hom} \tag{1.14}$$

With the restrictions

$$\begin{aligned} n_i &= n_{i\alpha} + n_{i\beta} + n_{io} \quad , \quad i = 1,2 \\ V &= V_\alpha + V_\beta \end{aligned} \tag{1.15}$$

and the notation $\tilde{n}_{i\alpha} = n_{i\alpha} + n_{io}$ we find for ΔF using eqs. (1.1)-(1.5) /4,5/:

$$\begin{aligned} \Delta F = {} & (p_\beta - p_\alpha) V_\alpha + \sigma A + \sum_{i=1}^{2} (\mu_{i\alpha} - \mu_{i\beta}) \tilde{n}_{i\alpha} \\ & + (p - p_\beta) V + \sum_{i=1}^{2} (\mu_{i\beta} - \mu_i) n_i \end{aligned} \tag{1.16}$$

ΔF (eq. 1.16) is known to be the reversible work of formation of a nucleus in a initially homogeneous binary system. The terms $(p-p_\beta)$ and $(\mu_{i\beta}-\mu_i)$ consider the change of the medium by the formation of the nucleus which is a typical effect for finite systems /2,4/.

The consistency with Gibbs' thermodynamics requires that the surface area of the nucleus is unambiguously defined by the volume of the α-phase: $A = A(V_\alpha)$. Calculating the equilibrium states from the extremum condition $d\Delta F = 0$ we find therefore the three conditions:

$$\mu_{i\alpha} = \mu_{i\beta} \qquad i = 1,2 \tag{1.17}$$

$$P_\alpha - P_\beta = \sigma \frac{dA}{dV_\alpha} \tag{1.18}$$

It has been shown in a general thermodynamic analysis /5,13/ that the equilibrium states, determined by eqs. (1.17), (1.18), should be either states corresponding to a stable coexistence of the nucleus and the surrounding matrix phase leading to a minimum of the free energy, or unstable equilibrium states of a saddle-point type.

2. Work of formation for an incompressible binary cluster

In order to calculate the work of formation of the cluster and the equilibrium conditions we now make use of the common approximation of an incompressible spherical cluster /14/. For this case an additional relation between the volume and the mole numbers of the nucleus exists:

$$V_\alpha = \frac{4\pi}{3} r_\alpha^3 = v_{1\alpha} n_{1\alpha} + v_{2\alpha} n_{2\alpha} \tag{2.1}$$

Since we assume an nearly ideal mixture of both components (no volume mixing effects), the specific molar volumes $v_{i\alpha}$ of the two components in the nucleus are expressed by the values for the pure components $v_{i\alpha}^0$. Furthermore, for spherical clusters it yields $\partial A / \partial V_\alpha = 2\sigma / r_\alpha$, r_α being the cluster radius.

The chemical potential of the α-phase generally depends on the pressure p_α, the molar fraction $x_{i\alpha}$ of the i-th component in the nucleus and the temperature. A Taylor expansion of $\mu_{i\alpha}$

valid for sufficiently large clusters leads to:

$$\mu_{i\alpha}(p_\alpha, x_\alpha, T) = \mu_{i\alpha}(p_\beta, x_\alpha, T) + \left.\frac{\partial \mu_{i\alpha}}{\partial p_\alpha}\right|_{T_\alpha = T_\beta} [p_\alpha - p_\beta] + \ldots \qquad (2.2)$$

Neglecting derivatives of the second order and considering $\left(\frac{\partial \mu_{i\alpha}}{\partial p_\alpha}\right)_{T,x_\alpha} = v^0_{i\alpha}$ the work of cluster formation (eq. 1.16) with respect to eqs. (2.1), (2.2) is now obtained as follows:

$$\Delta F = \sum_{i=1}^{2} (\mu_{i\alpha}(p_\beta, x_{i\alpha}, T) - \mu_{i\beta}(p_\beta, x_{i\beta}, T) + \frac{2\sigma}{r_\alpha} v^0_{i\alpha}) n_{i\alpha}$$

$$+ (p - p_\beta) V + \sum_{i=1}^{2} (\mu_{i\beta}(p_\beta, x_{i\beta}, T) - \mu_i(p, x_i, T)) n_i \qquad (2.3)$$

Because of the additional condition (eq. 2.1) we find now from the extremum condition $d\Delta F = 0$ two instead of three equilibrium conditions for the binary heterogeneous system, given by:

$$\mu_{i\alpha}(p_\beta, x_\alpha, T) - \mu_{i\beta}(p_\beta, x_\beta, T) + \frac{2\sigma}{r_\alpha} v^0_{i\alpha} = 0 \qquad i = 1,2 \qquad (2.4)$$

Finally, we want to specify the chemical potentials of both phases for a particular heterogeneous system. As mentioned before the nucleus should represent an incompressible binary liquid phase, while the surrounding matrix phase is given by a binary ideal vapour. Thus it yields /12/:

$$\mu_{i\alpha}(p_\alpha, x_\alpha, T) = \mu_{i\alpha}(p_{oi}, T) + v^0_{i\alpha}(p_\beta - p_{oi}) + RT \ln(x_{i\alpha} f_{i\alpha}) \qquad (2.5)$$

$$\mu_{i\beta}(p_\beta, x_\beta, T) = \mu_{i\beta}(p_{oi}, T) + RT \ln \frac{p_\beta}{p_{oi}} + RT \ln x_{i\beta} \qquad (2.6)$$

p_{oi} is chosen to be the partial saturation pressure of component i over a flat binary liquid surface. $x_{i\alpha}$ and $x_{i\beta}$ are the molar fractions of components i in the α- or the β-phase. In a binary system it yields $x_{2\alpha} = 1 - x_{1\alpha}$. Moreover, due to the limitation of the total mole number $x_{i\beta}$ is a function of the variables of the nucleus:

$$x_{2\beta} = \frac{n_{2\beta}}{n_\beta} = \frac{n x_2 - \tilde{n}_a x_{2\alpha}}{n - \tilde{n}_\alpha} \quad , \quad x_{1\beta} = 1 - x_{2\beta} \qquad (2.7)$$

x_2 means the molar fraction of the initial homogeneous state: $x_2 = n_2/n$, $x_1 = 1-x_2$. The $f_{i\alpha}$ are corrections to the mole fraction $x_{i\alpha}$ caused by nonideality effects of the liquid mixture. For ideal mixtures we have $f_{i\alpha} = 1$, but it is easy to consider also symmetrical mixtures and mixtures of the Margules-type using special expressions for the $f_{i\alpha}$ /12/. p_β means the actual vapour pressure in the system. Assuming an ideal vapour we have

$$p_\beta = \frac{n_\beta}{V_\beta} RT = \frac{n-\tilde{n}_\alpha}{V-V_\alpha} RT \qquad (2.8)$$

Inserting the expressions for the chemical potentials into eq. (2.4) the equilibrium conditions for a binary heterogeneous system read finally:

$$\ln\frac{p_\beta x_{i\beta}}{p_{oi} x_{i\alpha} f_{i\alpha}} - \frac{v^o_{i\alpha}}{RT}(p_\beta - p_{oi}) = \frac{2\sigma}{r_\alpha}\frac{v^o_{i\alpha}}{RT} \qquad i = 1,2 \qquad (2.9)$$

The eqs.(2.9) represent a generalized form of the Kelvin equation known to be the equilibrium condition for an one-component vapour above a curved liquid surface /10,11/. But here the depletion of the vapour caused by the formation of the cluster in the finite system is considered. Because the vapour pressure p_β and the molar fraction x_β both depend on the cluster variables, more than one solution of the system of equations (2.9) should exist for the finite binary system. That means, in addition to the critical cluster state a stable coexistence between both phases should be possible, dependent on the thermodynamic constraints.

3. Work of formation for a cluster in a quasi-binary solution with elastic straints

The given results should be applied, now, to a case of practical importance: the segregation of a pure component within a binary supersaturated solid solution /15,16/. Assuming that only component 2 segregates purely in clusters ($x_\alpha \equiv x_{2\alpha} = 1$) the molar fraction of the matrix is given by

$$x_\beta \equiv x_{2\beta} = \frac{n_{2\beta}}{n_\beta} = \frac{nx-\tilde{n}_\alpha}{n-\tilde{n}_\alpha}, \quad 1-x_\beta \equiv x_{1\beta} \qquad (3.1)$$

with $x \equiv n_2/n$. Instead of the constraints (1.13), we consider in the following:

$$n = \text{const.}, \; p = \text{const.}, \; T = \text{const.} \tag{3.2}$$

that means that the pressure p_β is always equal to the external pressure p. The thermodynamic potential for the given constraints (3.2) is the free enthalpy G. The work of cluster formation ΔG is found from eq. (2.3) considering $p_\beta = p$:

$$\Delta G = (\mu_{2\alpha}(p,x_\alpha,T)-\mu_{2\beta}(p,x_\beta,T)+\frac{3\sigma}{r_\alpha}v^o_{i\alpha})\tilde{n}_{2\alpha} + \sum_{i=1}^{2}(\mu_{i\beta}(p,x_{i\beta},T)-\mu_i(p,x_i,T))n_i \tag{3.3}$$

Replacing now the pressure p = const. by the concentration c = n/V = const. and neglecting a small term of the order $\sim v^o_{2\alpha}\cdot p$ the differences of the chemical potentials can be expressed in accordance with eqs. (2.5), (2.6) by:

$$\mu_{2\alpha} - \mu_{2\beta} \approx - RT \ln \frac{cx_\beta}{c_{2eq}} \tag{3.4}$$

$$\mu_{1\beta} - \mu_1 = RT \ln \frac{1-x_\beta}{1-x}, \quad \mu_{2\beta} - \mu_2 = RT \ln \left(\frac{x_\beta}{x}\right) \tag{3.5}$$

c_{2eq} means the saturation concentration of component 2 in the matrix which depends on temperature as follows:

$$\frac{1}{c_{2eq}} \frac{dc_{2eq}}{dT} = \frac{q}{RT^2} \tag{3.6}$$

q being the molar solution heat.
Inserting eqs. (3.4), (3.5) in eq. (3.3) we finally arrive at:

$$\frac{\Delta G}{RT} = (-\ln \frac{cx_\beta}{c_{2eq}} + \frac{3\sigma}{r_\alpha} v^o_{2\alpha})\,\tilde{n}_{2\alpha} + (x \ln \frac{x_\beta}{x} + (1-x) \ln \frac{(1-x_\beta)}{(1-x)})n \tag{3.7}$$

Eq. (3.7) takes into account the depletion of component 2 in the matrix due to the cluster formation by the change of x_β compared with x. If this depletion could be neglected as was assumed in the classical approximations, $x_\beta = x$ results and only the first

contribution to ΔG (eq. 3.7) remains.

We want to describe in the following the formation of AgCl-clusters in a silver halogenide /natrium borate solution. It should be realistic for this phase transition to consider also elastic strains /15,16/. These strains evolve when the matrix building units (components 1 and 2) change their places with these of the segregating units (component 2) which move to form the cluster, because the components 1 and 2 have a distinct mean molar volume. Assuming a spherical cluster phase α with an elastic modulus E and a Poisson number γ similar to the β-phase, the elastic strains can be described by equations of the Nabarro type /1/, that means the work of cluster formation eq. (3.7) is completed by an additional term

$$\Delta G^e = \varepsilon V_\alpha = \varepsilon v^o_{2\alpha} \tilde{n}_{2\alpha} \qquad (3.8)$$

which reflects the elastic energy, ε being

$$\varepsilon = \frac{E}{9(1-\gamma)} \delta^2 \; ; \quad \delta = \frac{\bar{v}_\beta - \bar{v}_\alpha}{\bar{v}_\alpha}$$

$\bar{v}$ stands for the mean molar volume of the considered phase. It yields:

$$\bar{v}_\alpha = v^o_{2\alpha}$$

$$\bar{v}_\beta = \frac{v_{1\beta} n_{1\beta} + v_{2\beta} n_{2\beta}}{n_{1\beta} + n_{2\beta}} = v_{1\beta}(1-x_\beta) + v_{2\beta} x_\beta \qquad (3.9)$$

Assuming an ideal mixture, the partial molar volumes $v_{i\beta}$ of the β-phase are given by the corresponding values of the pure components, $v^o_{i\beta}$, in the β-phase. Further, we note, that the molar fraction of the segregating component is rather small in the considered case, x = 0.02. Therefore we can approximate:

$$\bar{v}_\beta \approx v^o_{1\beta} \; ; \quad \delta \approx \frac{v^o_{1\beta} - v^o_{2\alpha}}{v^o_{2\alpha}} \qquad (3.10)$$

The influence of the elastic energy on the work of cluster formation is presented in Fig. 1 by the difference between the curves (b) and (c). It is shown that in the presence of elastic strains the nucleation barrier (maximum of ΔG) increases, fur-

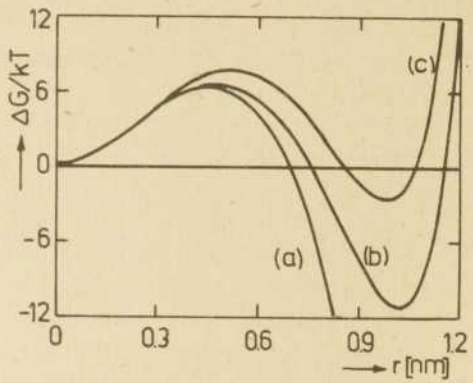

Fig. 1:
Free enthalpy ΔG ($k_B T$) (eq. 3.7) vs. cluster radius r (nm)
(a) neglecting depletion ($x_\beta = x$), (b) considering depletion, (c) considering depletion and elastic strains (eq. 3.8)

The calculation was carried out for a silver halogenide/natrium borate solution, x(AgCl) = 0.02, T = 820 K, $\xi = 7 \cdot 10^7$ N/m^2, total particle number N = 10^4, c = $3{,}48 \cdot 10^4$ mol/m^3

thermore, the critical cluster size increases too, and the stable cluster size indicated by a minimum of ΔG, decreases. The difference between the curves (a) and (b) demonstrates that a stable state is obtained only if the depletion of the segregating particles is considered. In the case $x_\beta = x$ we find only a critical cluster size which is smaller than before, and a lower nucleation barrier.

The influence of the elastic strains on the equilibrium states of the cluster shall be further discussed. By means of the extremum condition $\partial \Delta G / \partial n_{2\alpha} = 0$ we find the equilibrium condition:

$$\ln \frac{c x_\beta}{c_{2eq}^{(1)}} - \xi \frac{v_{2\alpha}^0}{RT} - \frac{2\sigma}{r_\alpha} \frac{v_{2\alpha}^0}{RT} = 0 \qquad (3.11)$$

The value $y = c x_\beta / c_{2eq}$ gives a measure of the actual supersaturation of component 2 in the system. Because x_β depends on r_α (eq. 3.1), we find two solutions of the equilibrium condition in a certain range of the temperature. Fig. 2 demonstrates the influence of the elastic strains on these states. For a given temperature the smaller value of the radius corresponds to the cri-

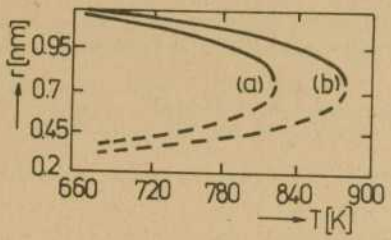

Fig. 2: Critical (---) and stable (——) cluster radius (nm) vs. temperature (K), (a) $\varepsilon = 7 \cdot 10^7$ N/m^2, (b) $\varepsilon = 0$
T_c is obtained as (a) 824 K, (b) 882 K
For the parameters see Fig. 1.

tical cluster size, while the larger value gives the stable cluster size. It is shown that the elastic strains decrease the stable cluster size and increase the critical cluster size. That means, in the presence of elastic strains the initial supersaturation in the system, given by the ratio cx/c_{2eq}, should be larger to form a cluster of the same critical size as in the case $\varepsilon = 0$.

The intersection of the stable and the critical cluster size for a certain temperature T_c indicates the smallest stable cluster in equilibrium with the surrounding phase. For $T > T_c$ a phase coexistence is thermodynamically impossible, that means for given constrains n = const., x = const., T_c is the upper limit of the temperature where a phase transition can occur in the system. This critical temperature for the phase transition depends on the value of the elastic strains as shown in Fig. 2. T_c becomes considerably smaller in the presence of elastic strains. This fact should be important for the determination of the appropriate values of the thermodynamic constraints for the phase transition in a binary solid solution.

References

1. Ulbricht, H.; Schmelzer, J.; Mahnke, R.; Schweitzer, F.: Thermodynamics of Finite Systems and the Kinetics of First-Order Phase Transitions, Teubner, Leipzig 1988
2. Schmelzer, J.; Schweitzer, F.: Z.phys.Chem. (Leipzig) 266

(1985) 943
3. Schweitzer, F.; Schimansky-Geier, L.: J.Colloid Interface Sci. 119 (1987) 67
4. Schmelzer, J.: Wiss. Zeitschrift WPU Rostock NR 34, 1 (1985) 39
5. Schmelzer, J.; Schweitzer, F.: Wiss. Zeitschrift WPU Rostock NR 37 (1988)
6. Schmelzer, J.: Z.phys.Chem. 266 (1985) 1057, 1121
7. Schmelzer, J.; Schweitzer, F.: Ann.Phys. (Leipzig) 44 (1987) 293
8. Schmelzer, J.; Schweitzer, F.: J.Non-Equilib.Thermodyn. 12 (1987) 255
9. Schmelzer, J.: Wiss. Zeitschrift WPU Rostock NR 33, 3 (1984) 40
10. Rusanov, A.I.: Phasengleichgewichte und Grenzflächenerscheinungen, Akademie-Verlag, Berlin 1978
11. Prigogine, I.; Bellemans, A.: Statistical Mechanics of Surface Tension and Adsorption, New York 1980
12. Kortüm, G.: Einführung in die chemische Thermodynamik, Göttingen 1963
13. Schweitzer, F.; Schmelzer, J.: Rostocker Physik.Manuskr. 10 (1987) 32
14. Wilemsky, G.: J.Chem.Phys. 62 (1975) 3763
15. Gutzow, I.; Schmelzer, J.; Pascova, R.; Popow, B.: Rostocker Physik. Manuskr. 8 (1985) 22
16. Schmelzer, J.; Gutzow, I.: Wiss. Zeitschrift WPU Rostock NR 35, 4 (1986) 5

Author:

Dr.rer.nat. Frank Schweitzer
Wilhelm-Pieck-Universität Rostock
Sektion Physik
Universitätsplatz 3
Rostock
DDR - 2500

Rostocker Physikalische Manuskripte, Heft 12 (1988)

Frank Schweitzer; Jürn Schmelzer

Critical Composition for Nucleation in Quasi-Binary Finite Systems

A first-order phase transition may proceed via homogeneous nucleation only in a certain range of the thermodynamic parameters /1/. From classical nucleation theory, e.g., the existence of a critical supersaturation is known, which must be reached, at least, in an infinite system, to observe the formation of drops /2/.

As was shown in recent investigations in finite systems we find, in addition, critical system volumes, critical total particle numbers or critical values of the temperatures, different from macroscopic ones, which determine the boundaries in the parameter space, for which homogeneous nucleation may occur /3/. These preceding investigations of critical thermodynamic parameters have been carried out mainly for one-component systems /3, 4/. But also for nucleation in a quasi-binary system the existence of a critical system volume /5/ and a critical temperature (in the foregoing paper /6/) have been discussed.

The investigations are extended now to the calculation of a critical initial composition of the quasi-binary system in dependence on temperature which must be reached at least to allow the formation of supercritical clusters.

1. The free enthalpy of cluster formation in dependence on the molar fraction

The system considered here is a supersaturated solid solution with two components under the thermodynamic constraints

$$n = \text{const.},\ p = \text{const.},\ T = \text{const.} \qquad (1.1)$$

Taking into account $n = n_1 + n_2$, we define the molar fraction of the initially homogeneous supersaturated system by $x = n_2/n$, n being the total mole number of the finite system, p the ex-

ternal pressure and T the temperature. The formation of clusters of a new phase results in the evolution of a heterogeneous system, consisting of clusters in the otherwise homogeneous matrix. Parameters, describing the cluster phase are specified further by α, parameters of the matrix by β .

Assuming, now, in addition, that the cluster is formed only by particles of component 2 (quasi-binary system) ($x_\alpha = 1$) and considering the cluster phase as incompressible ($v^o_{2\alpha}$ = constant) and of spherical shape, the number of particles in a cluster $\tilde{n}_{2\alpha}$ can be expressed through the radius r_α and the molar volume by $\tilde{n}_{2\alpha} = \frac{4\pi}{3} r_\alpha^3 / v^o_{2\alpha}$. The medium is considered as an ideal mixture of both components, the molar fraction being defined as

$$x_\beta = \frac{n_{2\beta}}{n_\beta} = \frac{n_2 - \tilde{n}_\alpha}{n - \tilde{n}_\alpha} = \frac{nx - \tilde{n}_\alpha}{n - \tilde{n}_\alpha} \tag{1.2}$$

The work of cluster formation is then given by the change of the free enthalpy connected with the transition from the initially homogeneous to the heterogeneous state. It has been derived in the foregoing paper /6/ as

$$\frac{\Delta G}{RT} = \left(-\ln \frac{c x_\beta}{c_{2eq}} + \frac{3\sigma}{r_\alpha} v^o_{2\alpha}\right) \tilde{n}_{2\alpha} + \left(x \ln \frac{x_\beta}{x} + (1-x) \ln \frac{(1-x_\beta)}{(1-x)}\right) n \tag{1.3}$$

Here c is the initial concentration of the total mole number, c_{2eq} the saturation concentration of component 2 in the matrix, $v^o_{2\alpha}$ the molar density of the particles in the cluster, σ the surface tension. The existence of elastic strains resulting from the formation of the cluster in the matrix is not considered here, it leads to an additional contribution to ΔG /6,7/.

Fig. 1 presents ΔG vs. the cluster radius r_α for different values of the initial molar fraction x of the binary system. First we note the existence of a critical cluster size given by a maximum of ΔG, and a stable cluster size where the free enthalpy has got a minimum. This stable state is caused by the depletion of the medium due to the cluster formation, because of n = const.

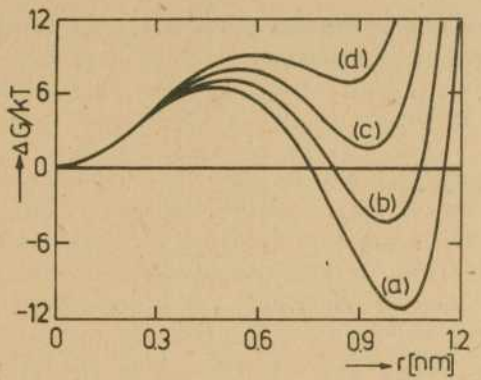

Fig. 1: Free enthalpy $\Delta G/k_B T$ (eq. 1.3) vs. cluster radius r_α (nm) (a) x = 0.02, (b) x = 0.019, (c) x = 0.018, (d) x = 0.017, the calculation was carried out for a silver halogenide/ natrium borate solution, x = x(AgCl), T = 820 K, c = $3.48 \cdot 10^4$ mol/m^3, total particle number N = 10^4

The values of the extrema of ΔG and the equilibrium cluster sizes both depend on the value of x. As shown in Fig. 1 we find a critical initial molar fraction x_c where ΔG has no extrema but only a point of inflexion. That means physically that for $x < x_c$ no supercritical resp. no stable cluster can exist in the system, and a phase separation by nucleation should be impossible from a thermodynamic point of view.

2. Equilibrium cluster sizes and critical molar fraction

The dependence of the extremum states on the initial composition x can be discussed in more detail calculating the equilibrium condition. We find for the first derivative of ΔG:

$$\left.\frac{\partial \Delta G}{\partial r_\alpha}\right|_x = -4\pi r_\alpha^2 \left[\frac{RT}{v_{2\alpha}^0} \ln \frac{c x_\beta}{c_{2eq}} - \frac{2\sigma}{r_\alpha}\right] = 0 \qquad (2.1)$$

The first solution of eq. (2.1) is given by $r_\alpha = 0$, that means we have a stable matrix phase β where no cluster exists.

The critical and the stable cluster sizes can be obtained from the following equilibrium condition:

$$\ln \frac{c x_\beta}{c_{2eq}} = \frac{2\sigma}{r_\alpha} \frac{v^\circ_{2\alpha}}{RT} \qquad (2.2)$$

Here the value $y = c x_\beta / c_{2eq}$ gives a measure of the actual supersaturation of component 2 in the system. Because x_β depends on r_α, eq. (2.2) possesses two solutions for a certain range of thermodynamic constraints. This is demonstrated in Fig. 2 obtained from an iteration of eq. (2.2). For a given value of x the smaller value for the radius corresponds to the critical cluster size and the larger value to the stable cluster size /2,3/. It is shown that for a critical value x_c both solutions coincide, and for $x < x_c$ no solution of the equilibrium condition (2.2) exists. As can be seen from the figure this critical composition itself depends on temperature: for a larger temperature x_c also has got a larger value. The existence of a lower boundary of x, for which a decomposition may occur, is known from macroscopic phase diagrams. The important point, which is

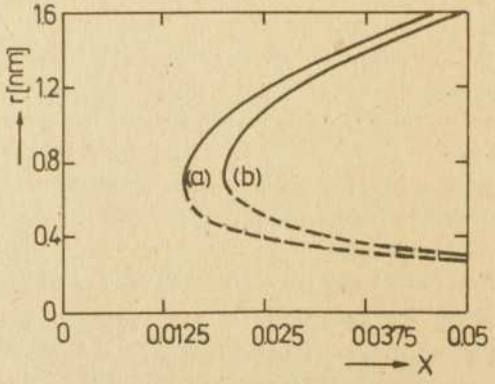

Fig. 2: Critical (---) and stable (——) cluster radius r_α (nm) vs. initial mole fraction x
(a) T = 800 K, (b) T = 880 K
x_c is obtained as (a) x_c = 0.0148, (b) x_c = 0.01995
For the parameters see Fig. 1.

to be stressed here, is the deviation of the corresponding value for finite compared with macroscopic systems. This result should be of importance in practical situations, if phase transitions in relatively small cavities are investigated. In the following this effect is studied in more detail.

Inserting x_β (eq. 1.7) into the equilibrium condition we find:

$$\ln \frac{c}{c_{2eq}} \frac{(nx - \frac{4\pi}{3} \frac{1}{v^o_{1\alpha}} r_\alpha^3)}{(n - \frac{4\pi}{3} r_\alpha^3 / v^o_{2\alpha})} - \frac{2\sigma}{r_\alpha} \frac{v^o_{2\alpha}}{RT} = 0 \qquad (2.3)$$

For the logarithm of eq. (2.3) we use a power expansion neglecting terms of higher than the first order. Then eq. (2.3) can be transformed into an algebraic equation for r_α /3,8/:

$$r_\alpha^4 + A\, r_\alpha + B = 0 \qquad (2.4)$$

with

$$A = -n(4\pi/\beta \cdot v^o_{2\alpha}))^{-1} \left(\frac{x}{1-x}\right)\left(\ln \frac{cx}{c_{2eq}}\right) < 0 \qquad (2.5)$$

$$B = n(4\pi/\beta \cdot v^o_{2\alpha}))^{-1} \left(\frac{1}{1-x}\right)\left(\frac{2\sigma v^o_{2\alpha}}{RT}\right) > 0 \qquad (2.6)$$

It has been shown analytically /8/ that eq. (2.4) possesses only two positive solutions which depend on the values of the thermodynamic constraints (compare also Fig. 2). These solutions coincide if the relation (2.7) holds

$$\left(\frac{A}{4}\right)^4 = \left(\frac{B}{3}\right)^3 \qquad (2.7)$$

Thus eq. (2.7) determines the boundaries in the space of the thermodynamic parameters between thermodynamically stable and metastable states. From eq. (2.7) we find with (2.5), (2.6):

$$n\left(\frac{x}{1-x}\right)\left(\ln \frac{cx}{c_{2eq}(T)}\right)^4 = 4\left(\frac{4\pi}{3v^o_{2\alpha}}\right)\left(\frac{4\pi}{3} \frac{2\sigma v^o_{2\alpha}}{RT}\right)^3 = \text{const.}(T) \qquad (2.8)$$

Neglecting the dependence of σ on the composition of the matrix, the r.h.s. of eq. (2.8) is only a function of temperature. For a given total particle number n in the system and a given temperature we can calculate, now, the critical value of x determined by eq. (2.8) The results are given in Fig. 3 for different va-

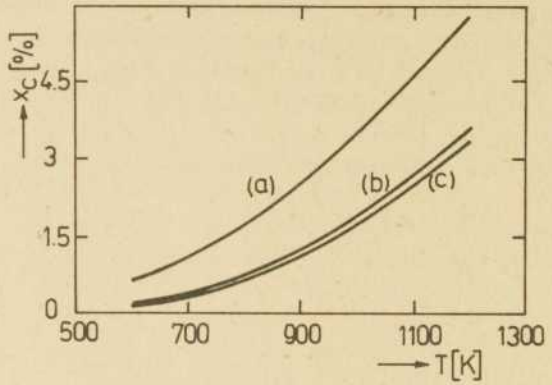

Fig. 3: Critical initial mole fraction x_c (%) vs. temperature (K), total particle number (a) $N = 10^4$, (b) $N = 10^8$, (c) $N > 10^{20}$
For the parameters see Fig. 1.

lues of n. Only for $x > x_c$ a phase transition via nucleation may occur. It is shown, that for finite systems x_c increases for a decreasing total mole number, but in the thermodynamic limit x_c converges into the constant value obtained for the infinite system.

3. Temperature dependence of the critical molar fraction

To obtain general analytical results concerning the temperature dependence of the critical value of the initial molar fraction x_c we apply, now, the theory of implicite functions in an analogous way, as it was done in an analysis of the size dependence of a critical temperature in one-component systems /10/.

As it was discussed in the preceding paragraphs (see, in particular, Fig. 1) the critical value of the molar fraction is given by the conditions (3.1)

$$\left.\frac{\partial \Delta G}{\partial r_\alpha}\right|_{x_c} = \frac{\partial^2 \Delta G}{\partial r_\alpha^2} = 0 \qquad (3.1)$$

The first derivative of ΔG is given by eq. (2.1). The second derivative can be calculated as follows:

$$\frac{\partial^2 \Delta G}{\partial r_\alpha^2} = -8\pi r_\alpha \left[\frac{RT}{v_{2\alpha}^o} \ln \frac{cx_\beta}{c_{2eq}} - \frac{2\sigma}{r_\alpha}\right] - 4\pi r_\alpha^2 \left[\frac{RT}{v_{2\alpha}^o} \frac{1-x_\beta}{n_\beta x_\beta} (-4\pi r_\alpha^2 / v_{2\alpha}^o) + \frac{2\sigma}{r_\alpha^2}\right] \tag{3.2}$$

We obtain therefore the following system of equations for the determination of x_c

$$f_1(r_\alpha, n, x, T) = \ln \frac{cx_\beta}{c_{2eq}} - \frac{2\sigma}{r_\alpha} \frac{v_{2\alpha}^o}{RT} = 0$$

$$f_2(r_\alpha, n, x, T) = -4\pi r_\alpha^3 / v_{2\alpha}^o \frac{1-x_\beta}{n_\beta x_\beta} + \frac{2\sigma}{r_\alpha} \frac{v_{2\alpha}^o}{RT} = 0 \tag{3.3}$$

For a given value of n both equations define implicitely a function r_α (x,T). Combining these two functions, we find an equation for $x_c(T)$. A numerical solution of the system of equations (3.3) is possible, it is equivalent to the results, given in Fig. 2, obtained based on eqs. (2.3) and (2.7).

Based on eqs. (3.3) and the theory of implicite functions we may obtain the following differential equations for the cluster size r_α^c, corresponding to the point of inflexion, and the critical molar fraction x_c in dependence on temperature.

$$\frac{dr_\alpha^c}{dT} = -\frac{1}{\Delta} \begin{vmatrix} \frac{\partial f_1}{\partial T} & \frac{\partial f_1}{\partial x} \\ \frac{\partial f_2}{\partial T} & \frac{\partial f_2}{\partial x} \end{vmatrix} \tag{3.4}$$

$$\frac{dx_c}{dT} = -\frac{1}{\Delta} \begin{vmatrix} \frac{\partial f_1}{\partial r_\alpha} & \frac{\partial f_1}{\partial T} \\ \frac{\partial f_2}{\partial r_\alpha} & \frac{\partial f_2}{\partial T} \end{vmatrix} \tag{3.5}$$

with

$$\Delta = \begin{vmatrix} \frac{\partial f_1}{\partial r_\alpha} & \frac{\partial f_1}{\partial x} \\ \frac{\partial f_2}{\partial r_\alpha} & \frac{\partial f_2}{\partial x} \end{vmatrix} \tag{3.6}$$

The partial derivatives of the functions f_1 and f_2 (eqs. 3.3) are calculated approximately, retaining only the dominant terms. Consequently, the possible temperature dependence of σ, $v^o_{2\alpha}$ is neglected, c_{2eq} is expressed through /11/

$$\frac{1}{c_{2eq}} \frac{\partial c_{2eq}}{\partial T} = \frac{q}{RT^2}$$

q being the molar heat of solution.

This approach yields

$$\frac{\partial f_1}{\partial T} \approx - \frac{q}{RT^2} \qquad \frac{\partial f_2}{\partial T} = - \frac{2\sigma v^o_{2\alpha}}{RT^2} \frac{1}{r_\alpha}$$

$$\frac{\partial f_1}{\partial x} = - \frac{1}{x_\beta} \frac{n}{n_\beta} \qquad \frac{\partial f_2}{\partial x} = \frac{4\pi r_\alpha^3}{v^o_{2\alpha} n_\beta x_\beta^2}$$

$$\frac{\partial f_1}{\partial r_\alpha} \approx \frac{2\sigma v^o_{2\alpha}}{RT} \frac{1}{r_\alpha^2} \qquad \frac{\partial f_2}{\partial r_\alpha} \approx - \frac{2\sigma v^o_{2\alpha}}{RT} \frac{1}{r_\alpha^2}$$

Inserting these derivatives into eqs. (3.5), (3.6) the dependence of the critical molar fraction on temperature can be expressed by

$$\frac{dx^c}{dT} = \frac{n_\beta x_\beta^2 \left[\frac{q}{RT^2} + \frac{2\sigma v^o_{2\alpha}}{RT^2} \frac{1}{r_\alpha} \right]}{4\pi r_\alpha^3 / v^o_{2\alpha} + n x_\beta} \tag{3.7}$$

For a discussion of eq. (3.7) we approximate, finally, the derivative again by the largest terms of the numerator and the denominator and arrive at:

$$\frac{dx^c}{dT} \approx \frac{n_\beta x_\beta}{n} \frac{q}{RT^2} \tag{3.8}$$

In agreement with the numerical results presented in Fig. 3 we find that the critical initial molar fraction x_c increases with an increasing temperature or, in other words, with a decreasing initial supersaturation. The temperature dependence of x_c can be given also in an alternative form obtained from eq. (3.8)

$$\frac{dx_c}{dT} = \left(\frac{1}{c_{2eq}} \frac{\partial c_{2eq}}{\partial T} \right) \left(\frac{1}{x_\beta} \frac{\partial x_\beta}{\partial x} \right)^{-1} \tag{3.9}$$

It means that the most important contributions to the change of x_c with temperature are the temperature dependence of c_{2eq} and the dependence of x_β on x reflecting the influence of the total number of particles n.

References

1. Ulbricht, H.; Schmelzer, J.; Mahnke, R.; Schweitzer, F.: Thermodynamics of Finite Systems and the Kinetics of First-Order Phase Transitions, Teubner, Leipzig 1988
2. Becker, R.; Döring, W.: Ann.Phys. 24 (1935) 719
3. Schweitzer, F.; Schimansky-Geier, L.: J.Colloid Interface Sci. 119 (1987) 67
4. Schmelzer, J.; Schweitzer, F.: Z.phys.Chem. (Leipzig) 266 (1985) 943
5. Schmelzer, J.; Schweitzer, F.: Ann.Phys. (Leipzig) 44 (1987) 283
6. Schweitzer, F.: Rostocker Physik. Manuskr. 12 (1988)50
7. Gutzow, I.; Schmelzer, J.; Pascova, R.; Popov, B.: Rostocker Physik. Manuskr. 8 (1985) 22
8. Schweitzer, F.; Ulbricht, H.; Schmelzer, J.: Wiss.Zeitschr. WPU Rostock NR 33, 4 (1984) 45, 54
9. Fichtenholz, G.M.: A Course in Differential and Integral Calculus, Moscow 1966 (in Russian)
10. Schmelzer, J.; Schweitzer, F.: submitted to Z.phys.Chem.
11. Kortüm, G.: Einführung in die chemische Thermodynamik, Göttingen 1963

Authors:

Dr.rer.nat. Frank Schweitzer
Doz. Dr.sc.nat. Jürn Schmelzer
Wilhelm-Pieck-Universität Rostock
Sektion Physik
Universitätsplatz 3
Rostock
DDR - 2500

Rostocker Physikalische Manuskripte, Heft 12 (1988)

Frank Schweitzer; Jörn Bartels

The Effect of Elastic Strains and Depletion on Nucleation and Growth in Binary Solutions

As discussed in preceding papers /1,2/ elastic strains quantitatively and qualitatively modify the kinetics of growth of the supercritical clusters and the cluster evolution in the late stage of Ostwald ripening.

In this paper we restrict ourselves mainly to the initial stage of the phase transition including the formation of clusters and their growth up to an overcritical size.

The investigations are based on a thermodynamic analysis presented in the foregoing papers /3,4,5/.

1. Rate equation

We consider a binary system with the thermodynamic constraints

$$n = n_1 + n_2 = \text{const.}, \; p = \text{const.}, \; T = \text{const.} \qquad (1.1)$$

where n is the total mole number in the system consisting of two components, p the external pressure and T the temperature. The molar fraction of the initial stage is introduced as $x = n_2/n$. In the heterogeneous state the total mole number is divided into the mole number of the cluster phase, denoted by α, and the mole number of the matrix phase indicated by β. Assuming as before /4,6,7/, that the clusters are formed only by particles of component 2 it yields $n_2 = n_{2\beta} + n_\alpha = \text{const.}$ and we may write for the molar fraction of the matrix:

$$x_\beta = \frac{n_{2\beta}}{n_\beta} = \frac{nx - n_\alpha}{n - n_\alpha} \qquad (1.2)$$

The cluster phase shall be spatially distributed in clusters with the particle number j ($j \geq 2$)

$$n_\alpha = N_A^{-1} \sum_{j=2}^{N} j N_j \,, \qquad (1.3)$$

N_j being the number of clusters of size j and N_A the Avogadro number. Denoting the particle number of component 2 of the matrix by N_1 (that means free particles) it yields

$$n_{2\beta} = N_A^{-1} N_1 \tag{1.4}$$

and we obtain the following continuous equation resulting from the conservation of particles in the system /8/

$$\frac{\partial N_1}{\partial t} = -\frac{\partial}{\partial t} \sum_{j=2}^{N} j N_j \tag{1.5}$$

The change of the number of clusters of size j with time can be described by a rate equation. Assuming like in classical nucleation theory /9/ that the growth of clusters occurs only by the attachment of free particles, neglecting collisions of larger clusters, and assuming further that the clusters shrink detaching single particles, the rate equation can be written in the form:

$$\frac{\partial N_j}{\partial t} = I_{j-1} - I_j \qquad j = 2,3,\ldots,N \tag{1.6}$$

I_j is the netto rate of formation of clusters of size j. It depends on time because the actual number of clusters of size j as well as the transition rates w^+ and w^- both depend on time:

$$I_j(t) = w_j^+(t) N_j(t) - w_{j+1}^-(t) N_{j+1}(t) \tag{1.7}$$

Eq. (1.6) represents a hierarchy of differential equations which must be solved successively to know the actual cluster distribution $N_i(t)$ (i=1,2,...,N). For a calculation we have to determine first the transition rates w^+ and w^-.

2. Equilibrium cluster distribution

In order to determine the transition rates we make use of the condition of detailled balance /8/. That means for finite systems in equilibrium the netto rate I_j (eq. 1.7) must vanish for every j, resulting in:

$$w_j^+ N_j^0 = w_{j+1}^- N_{j+1}^0 \tag{2.1}$$

N_j^o denotes the equilibrium cluster distribution which can be obtained from a mass action law by:

$$N_j^o = N_1 \exp\left\{-\frac{\Delta G_j}{k_B T}\right\} \tag{2.2}$$

$N_1 = N_A \cdot n_2$ gives the normalization. ΔG_j is the Gibbs free energy to form a cluster of size j (not the thermodynamic potential of the whole system). It is given by /9/

$$\Delta G_j = -\Delta g \cdot j + \sigma \cdot j^{2/3} \tag{2.3}$$

The first term of eq. (2.3) describes the binding energy in the cluster (bulk phase), the second term the surface energy caused by the formation of a (spherical) surface with the surface tension σ. The binding energy per particle in the cluster can be approximated classically by /9/:

$$\frac{\Delta g}{k_B T} = \ln \frac{cx}{c_{2eq}(T)} \tag{2.4}$$

Here c is the total particle density in the system being constant, x is the initial molar fraction of component 2 and $c_{2eq}(T)$ is the equilibrium concentration of component 2 in the matrix depending on temperature by /10/

$$c_{2eq}(T) = c_{2eq}(T_o) \exp\left\{\frac{q}{k_B T}\left(\frac{1}{T_o} - \frac{1}{T}\right)\right\} \tag{2.5}$$

q means the solution heat per particle.
The ratio cx/c_{2eq} is a measure of the supersaturation in the classically infinite system.

For the finite system we have to consider firstly the depletion of the matrix, that means, x must be replaced by the actual molar fraction x_β /6,7/. Secondly, the existence of elastic strains caused by the cluster formation in the matrix decreases the effective supersaturation by a certain amount $\varepsilon v_{2\alpha}^o$, as has been discussed in the foregoing paper /4/. ε is a measure for the elastic strains. Assuming strains of a Nabarro-type /5/, ε depends only on the elastic modul, the Poissonian number, the molar volumes of the pure components 1,2, of the phases α and β (see /4/). $v_{2\alpha}^o$ is the molar volume of component 2 in the cluster. With respect to depletion and elastic strains in the con-

sidered system we introduce now instead of eq. (2.4):

$$\frac{\Delta g^e}{k_B T} = \ln \frac{c x_\beta}{c_{2eq}(T)} - \varepsilon \frac{v^o_{2\alpha}}{k_B T} \qquad (2.6)$$

Considering the temperature dependence of c_{2eq} (eq. 2.5) we arrive at:

$$\frac{\Delta g^e}{k_B T} = \ln \frac{c x_\beta}{c_{2eq}(T_o)} - \frac{q}{k_B T}\left(\frac{T-T_o}{T_o}\right) - \frac{\varepsilon v^o_{2\alpha}}{k_B T} \qquad (2.7)$$

In the following Δg^e (eq. 2.7) gives a measure of the effective actual supersaturation in the system in contrast to the initial supersaturation (eq. 2.4).

The formation energy ΔG_j (eq. 2.3) has got a maximum for the critical cluster size $r \sim j^{1/3}$:

$$r_{cr} = \frac{2\sigma v^o_{2\alpha}}{k_B T}\left(\ln \frac{c x_\beta}{c_{2eq}(T)} - \frac{\varepsilon v^o_{2\alpha}}{k_B T}\right)^{-1} = \frac{2\sigma v^o_{2\alpha}}{\Delta g^e (k_B T)^2} \qquad (2.8)$$

This equation for the critical radius r_{cr} agrees obviously with the equilibrium condition derived before /4/ for the considered system with respect to elastic strains.

3. Transition rates

Because the aquilibrium cluster distribution N^o_j is known, now, we need a kinetic assumption for one of the transition rates w^+, w^- in order to determine the transition rate for the opposite process from the condition of detailled balance /8/. We decide for an ansatz for the transition rate of attachment of free particles.

The Fickian law gives a relation between the flux of free particles through a spherical surface and the gradient of the concentration c_1 of free particles:

$$\frac{dN_1}{dt} = -D\, 4\pi R_j^2 \left.\frac{dc_1(r)}{dr}\right|_{r=R_j} \qquad (3.1)$$

Here R_j means the radius of the spherical cluster, r is the distance from the cluster and D the diffusion constant of free particles of component 2 in the matrix consisting of components

1 and 2. The gradient $\partial c_1 / \partial r$ must be determined from the diffusion equation

$$\Delta c_1(r) = 0 \tag{3.2}$$

We assume the boundary conditions

$$1.\ c_1(r \to \infty) = c_{2\beta} \quad 2.\ c_1(r=R_j) = 0 \tag{3.3}$$

The first condition reflects that the concentration of free particles apart from the cluster agrees with the actual concentration of component 2 in the matrix. The second condition means that all free particles which arrive at the cluster surface will be bound in the cluster - that is the meaning of the transition rate of attachment. With eqs. (3.3) we find from eq. (3.2):

$$c(r) = c_{2\beta}\left(1 - \frac{R_j}{r}\right) \tag{3.4}$$

Inserting this result into eq. (3.1) we arrive at:

$$\frac{dN_1}{dt} = - D\, 4\pi R_j\, c_{2\beta} \tag{3.5}$$

It seems to be sensible now to make the following ansatz for w_j^+ in agreement with the solution (3.5) of the Fickian law:

$$w_j^+ = \alpha D\, 4\pi r_j\, cx_\beta \tag{3.6}$$

cx_β means the actual concentration of free particles of component 2 in the matrix which form the clusters, $r_j \sim j^{1/3}$ is the cluster radius and α is a constant which scales the time and should reflect the properties of the surface, like surface tension, sticking coefficient and so on. Using the condition of detailled balance (eq. 2.1) with respect to eqs. (2.2), (2.3), (2.6) we find the transition rate for the detachment of free particles from the cluster in the form:

$$w_j^- = \alpha 4\pi D\, r_j c_{2eq} \exp\left[\left(\frac{2\sigma}{3k_B T}\, j^{-1/3}\right)\left(\frac{\varepsilon\, v_{2\alpha}^0}{k_B T}\right)\right] \tag{3.7}$$

We choose for the time the unknown parameter α to be arbitrary equal to one and introduce the capillary length $d_0 = 2\sigma v_{2\alpha}^0 / k_B T$ and the equilibrium concentration of free particles above the curved cluster surface by

$$c_{eq}(r_j) = c_{eq2}(T)\ \exp\left\{\frac{d_0}{r_j}\right\} \qquad (3.8)$$

After a division of the eqs. (3.6) and (3.7) by the constant $\exp(-\xi\, v^0_{2\alpha}/k_BT)$ the transition rates to describe the cluster growth and shrinkage with respect to elastic strains and to the depletion of the matrix are obtained finally in the form:

$$\begin{aligned} w_j^+ &= 4\pi D\, r_j\, c x_\beta\, \exp\left\{-\frac{\xi\, v^0_{2\alpha}}{k_BT}\right\} \\ w_j^- &= 4\pi D\, r_j\, c_{eq}(r_j) \end{aligned} \qquad (3.9)$$

In contrast to a classical description the transition rate of attachment of free particles depends on the whole cluster distribution because of the dependence on x_β. This fact has been obtained also in isochoric gases /8,11/. Because we have in the considered case a diffusion-controlled cluster growth (remember eq. (3.3) and $\alpha=1$) and not an interface-controlled growth like in isochoric gases, w^+ is here only proportional to r_j and not to r_j^2. Moreover, it becomes clear that elastic strains decrease the transition rate of cluster growth to a certain extent and the clusters will form slowlier.

4. Deterministic growth equation for supercritical clusters

It is known from stochastic simulations of the nucleation process /8/ that for clusters with an overcritical size the probability to shrink becomes smaller compared with the one describing the further growth. Therefore, the evolution of overcritical clusters can be well described by a deterministic growth equation which neglects the probability of shrinkage of supercritical clusters. For the evolution of the cluster distribution then the following Liouville equation is held /12/

$$\frac{\partial N_j}{\partial t} = -\frac{\partial}{\partial j}\,(N_j v_j) + I_j(t) \qquad (4.1)$$

Here I_j denotes a source term which agrees in the considered case with the netto rate (eq. 1.7) of cluster formation. The first term of the r.n.s. reflects the deterministic cluster growth and shrinkage. v_j means the deterministic velocity which can be derived from /12/

$$v_j = \frac{dj}{dt} = w_j^+ - w_j^- \qquad (4.2)$$

Inserting the known transition rates w^+, w^- (eq. 3.9) it yields for the considered case:

$$v_j = 4\pi D\, r_j \left[c x_\beta \exp\left(-\frac{\varepsilon v_{2\alpha}^o}{k_B T}\right) - c_{2eq} \exp\left(\frac{d_o}{r_j}\right)\right] \qquad (4.3)$$

Use of power expansion for the exponential functions up to the first order leads to:

$$v_j = 4\pi D\, r_j c_{2eq} \left[\ln \frac{c x_\beta}{c_{2eq}(T)} - \frac{\varepsilon v_{2\alpha}^o}{k_B T} - \frac{d_o}{r_j}\right] \qquad (4.4)$$

Finally, we introduce the critical cluster size given by eq. (2.8) and arrive at the deterministic growth equation:

$$v_j = 4\pi D\, d_o\, c_{2eq}(T)\, r_j \left(\frac{1}{r_{cr}(t)} - \frac{1}{r_j}\right) \qquad (4.5)$$

In eq. (4.5) the critical radius $r_{cr}(t)$ (eq. 2.8) acts as an selection value. Only clusters with a radius r_j larger than r_{cr} are able to grow, clusters with a size $r_j < r_{cr}$ must shrink and diminish again. In contrast to classical nucleation theory the critical radius depends on time now, because x_β depends on time. It increases from an initial value

$$r_{cr}(t=0) = d_o \left(\ln \frac{cx}{c_{2eq}} - \frac{\varepsilon v_{2\alpha}^o}{k_B T}\right) \qquad (4.6)$$

which agrees with r_{cr} for the classical infinite system, up to the value of the stable cluster size (compare Fig. 2 in the foregoing paper /4/) and v_j becomes equal to zero in stable equilibrium.

Note that eq. (4.5) is related to known equations describing the selection of different species in self-organizing systems /5,13/. Deterministic equations for crystal growth in viscoelastic and elastic media derived from a quite different ansatz but in conclusion similar to eq. (4.5) are given in /1,2/.

In order to solve the kinetic equations (1.6), (1.7), (4.1) for nucleation and growth of clusters we use now the following boundary conditions:

(i) $N_j(t=0) = 0$ for $j \geq 2$; that means initially only free particles of component 2 exist in the system.
(ii) Clusters with a size $j > j^* > j_{cr}$ are no longer considered in terms of the rate equation. Classically their further growth will be neglected. We describe the cluster growth for $j > j^*$ by a deterministic growth equation (4.1) where for $j = j^*$ the source term is given by the netto rate $I_j(t)$ (eq. 1.7). For $j > j^*$ the source term results from the cluster growth only.
(iii) $N_j(t) = N_j^0$ for $j < u$, that means the cluster distribution is equal to the equilibrium distribution (eq. 2.2) up to a small cluster size u (about five particles).
(iv) The conservation of the total particle number of component 2 $\sum_{j=1}^{M} jN_j = \text{const.}$ is always fulfilled.
The given kinetic equations are applied now to cluster growth in a solid solution. The parameters are related to a silver halogenide/natrium borate solution where AgCl-clusters are formed, but we are not engaged here in a comparison between theory and experiment. Only the initial stage of the phase transition is investigated. For results in comparison with measurements for larger times we refer the reader to refs. /1,2,14/.

5. Solution of the kinetic equations

The investigation of nucleation and growth in the solid solution shall demonstrate
(i) the influence of the depletion of the matrix and
(ii) the influence of elastic strains
on the kinetics of phase transition during the first stage.
(i) The effect of depletion is demonstrated in Fig. 1 which presents the netto rates of cluster formation in the limit of vanishing elastic strains ($\varepsilon = 0$). Curve a is obtained considering a phase transition without any depletion as assumed in classical nucleation theory. In this case a stationary nucleation rate is established ($I_j = I_{j+1} = \ldots = I^s = \text{const.}$) which can be approximated by /9/:

$$I^s = \left\{ \sum_{j=1}^{j^*} \frac{1}{w_j^+ N_j^0} \right\}^{-1} \approx I_0 \exp\left\{ \frac{4\pi}{3} \frac{\sigma}{k_B T} r_{cr}^2 \right\} \qquad (5.1)$$

I_o is a constant (about 10^{31} $m^{-3}s^{-1}$) which is derived in classical nucleation theory /9/. r_{cr} means the critical radius being classically constant because the depletion is neglected. It is obtained from eq. (4.6) keeping in mind that in Fig. 1 $\xi = 0$. In a quasi-stationary approximation /5,15/ the classical formulae for the nucleation rate (eq. 5.1) is used, but now taking into account the depletion of the matrix by the already formed clusters. This results in a time dependence of the critical radius which is now given by eq. (2.8) with $\xi = 0$. Curve b (Fig. 1) presents the quasi-stationary nucleation rate. Caused by the depletion, a slight decrease of I is obtained in the initial stage of the phase transition.

But the quasi-stationary approximation still neglects the further growth of the already formed clusters. This effect increases the depletion of the matrix considerably, it predominates the depletion caused by the cluster formation only. Therefore, the nucleation process cannot longer be described as a stationary process. Instead of approximation (5.1) we now have

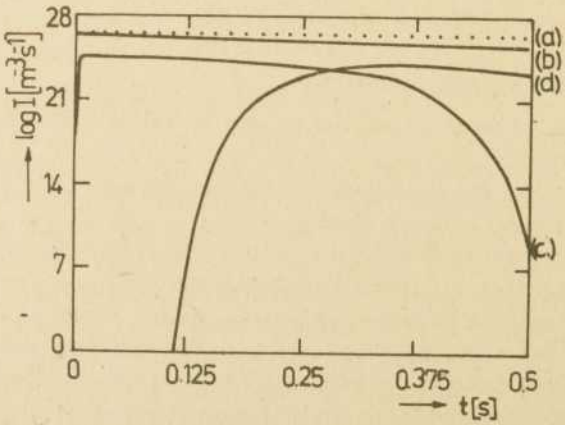

Fig. 1: Rate of cluster formation I (clusters/m^3s) in dependence on time (s)
(a) classical nucleation rate (eq. 5.1), (b) quasi-steady state approximation, (c) $I(j_{cr})$ (eq. 1.7), (d) I(j=250) (eq. 1.7)
The parameters are related to a silver halogenide/natrium borate solution, $c = 2.1 \cdot 10^{24} m^{-3}$, x = 0.02, T = 730 K, $\xi = 0$

to solve the system of rate equations (1.7) because both nucleation of critical clusters and growth of supercritical clusters depend reciprocally and should be described simultanously /15/. The nonstationary nucleation rate of critical clusters (cf. also /16/) is given in curve c (Fig. 1). After a certain time lag, known already from classical nucleation theory, $I(j_{cr})$ is nearly constant in a small range of the time - only for this range a steady state approximation should be satisfied.

But we note that I_{cr} is always smaller than the value given by the classical formulae. This fact can be understood only from a kinetic point of view: Because we start with a distribution of only free particles first during the time lag a metastable equilibrium cluster distribution is established which decreases in a very short time the initial supersaturation to a certain value /8/ (compare Fig. 3). Only this value gives the real "initial" supersaturation for the nucleation of critical clusters. The classical nucleation theory ignores this relaxation into the metastable state for a calculation of I^S. Curve c shows that $I(j_{cr})$ after a small time decreases rapidly caused by the depletion. Keep in mind, that in the same time the critical cluster size j_{cr} is increased, too.

Curve d of Fig. 1 gives the nucleation rate to form clusters with 250 particles. $I(j=250)$ is used to be the source term for the growth equation (4.1). Clusters with a size $j > 250$ are always supercritical for the considered times ($t \leq 0.7$ s), therefore, their further growth here is described by the deterministic growth equation. It is shown that the time lag to form clusters of 250 particles becomes much greater. As discussed before, also for $I(j=250)$ no stationary value could be obtained - after a certain time it decreases again (not clearly to be seen in Fig. 1.).

The largest cluster obtained in the system after $t = 0.64$ s has got a size of 1.9 nm that means nearly 2400 particles. It becomes clear that such a decrease of the free particles in the system should be not ignored in the initial stage of the phase transition.

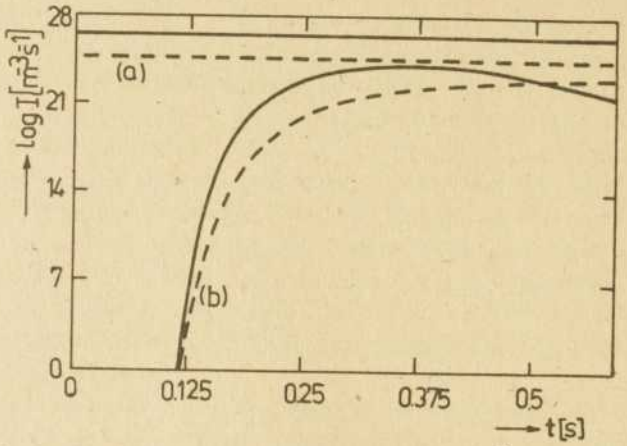

Fig. 2: Rate of cluster formation I (clusters/m^3s) in dependence on time (s)
(a) classical nucleation rate (eq. 4.1), (b) I(j=250) (eq. 1.7)
solid lines: $\varepsilon = 0$, dashed lines: $\varepsilon = 6.1 \cdot 10^7 Jm^{-3}$
For the parameters see Fig. 1.

(ii) In order to investigate the influence of elastic strains we calculate both the classical nucleation rate I^s = const. and the rate I(j=250) for two values of ε. The solid lines in Fig. 2 give the nucleation rates without elastic strains, the dashed lines consider elastic strains. The curves (a) represent the classical steady-state nucleation rate (eq. 5.1). It is shown that elastic strains decrease I^s considerably because the effective supersaturation $\Delta g^e/k_BT$ (eq. 2.7) becomes smaller in dependence on ε. In contrast to (a) the curves (b) give the non-stationary nucleation rate I(j=250) obtained from a solution of the system of rate equations (eqs. 1,6, 1.7). After the time lag the netto rate for $\varepsilon = 0$ increases faster, but also decreases earlier than the rate in presence of ε. This fact must be understood also kinetically:

Fig. 3 gives the effective supersaturation (eq. 2.7) in dependence on time. Because the initial concentration of free particles in the system, cx, is equal in both cases, the existence of elastic strains decreases the initial supersaturation compared with $\varepsilon = 0$. A lower supersaturation relaxes slowlier into its equilibrium value. This fact has been discussed also for

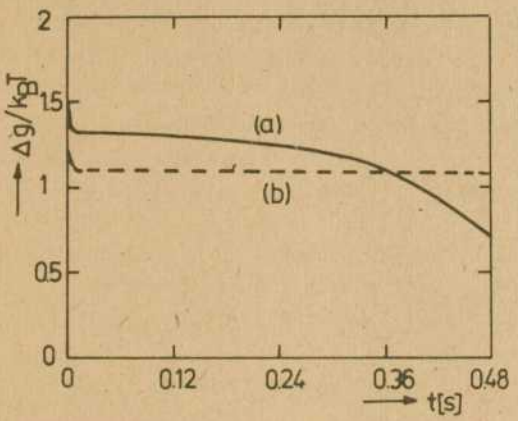

Fig. 3:
Effective supersaturation $\Delta g / k_B T$ (eq. 2.7) in dependence on time t (s), (a) $\varepsilon = 0$, (b) $\varepsilon = 6.1 \cdot 10^7$ Jm^{-3}
For the parameters see Fig. 1.

stochastic simulations of the nucleation process /8,5/. It becomes clear that after a certain time the supersaturation for $\varepsilon = 0$ is more decreased because it reduces faster and the nucleation rate becomes smaller compared with $\varepsilon > 0$. That means the period of formation of clusters becomes longer for systems where elastic strains exist, because the relaxation processes proceed slowlier.

We summarize the results for the kinetics of phase transition obtained for the first period, now, as follows:

1. In finite systems a depletion of the matrix is obtained caused by the formation of new clusters and the growth of already formed clusters. Therefore, the critical radius of cluster formation depends on time.

2. Since this depletion cannot be neglected, a nonstationary nucleation rate must be calculated from a system of rate equations. A deterministic growth equation describes the further growth of the already formed supercritical clusters.

3. The nucleation process of formation of critical clusters starts with a supersaturation smaller than the initial supersaturation, because the system first relaxes in a metastable equilibrium state.

4. Elastic strains lead to a decrease of the supersaturation. Smaller supersaturations relax slowlier into the equilibrium value, therefore, the nucleation period becomes longer in the presence of elastic strains.

References

1. Gutzow, I.; Schmelzer, J.; Pascova, R.; Popov, B.: Rostocker Physik. Manuskr. 8 (1985) 22
2. Schmelzer, J.; Gutzow, I.: Wiss.Zeitschr. WPU Rostock NR 35, 4 (1986) 5
3. Schmelzer, J.; Schweitzer, F.: Z.phys.Chem. (Leipzig) 266 (1985) 943
4. Schweitzer, F.: Rostocker Physik. Manuskr. 12 (1988) 50
5. Ulbricht, H.; Schmelzer, J.; Mahnke, R.; Schweitzer, F.: Thermodynamics of Finite Systems and the Kinetics of First-Order Phase Transitions, Teubner, Leipzig 1988
6. Schmelzer, J.; Schweitzer, F.: Ann.Phys. (Leipzig) 44 (1987) 283
7. Schmelzer, J.; Schweitzer, F.: J.Non-Equilib.Thermodyn. 12 (1987) 255
8. Schweitzer, F.; Schimansky-Geier, L.; Ebeling, W.; Ulbricht, H.: Physica A (1988) in press
9. Springer, G.S.: Adv.Heat Transfer 14 (1978) 281
10. Kortüm, G.: Einführung in die chemische Thermodynamik, Göttingen 1963
11. Schimansky-Geier, L.; Schweitzer, F.; Ebeling, W.; Ulbricht, H.: in: Selforganization by Nonlinear Irreversible Processes (Eds. W. Ebeling, H. Ulbricht), Springer, Heidelberg Berlin 1986, p. 67
12. Schweitzer, F.: Wiss.Zeitschr. WPU Rostock NR 35, H4 (1986)19
13. Mahnke, R.; Feistel, R.: Rostocker Physik.Manuskr. 8 (1985) 54
14. Lembke, U.; Mahnke, R.: Rostocker Physik.Manuskr. 8 (1985) 90
15. Schmelzer, J.; Ulbricht, H.: J.Colloid Interface Sci. 117 (1987) 325
16. Kelton, K.F.; Greer, A.L.; Thompson, C.V.: J.Chem.Phys. 79 (1983) 6261

Authors:

Dr.rer.nat. Frank Schweitzer
cand.phys. Jörn Bartels
Wilhelm-Pieck-Universität Rostock
Sektion Physik
Universitätsplatz 3
Rostock
DDR - 2500

Rostocker Physikalische Manuskripte, Heft 12 (1988)

Jürn Schmelzer

Growth Processes at Non-Spherical Interfaces and the Steady-State Approximation

1. Introduction

Segregation processes in multicomponent systems, in general, and binary systems, in particular, proceed usually by diffusion processes of, at least, one of the components. For a description of the growth of the new phase thus, in general, the following system of equations can be applied /1-3/:

$$\frac{dn_{i\alpha}}{dt} = -4\pi A \bar{j}_i \bar{e}$$

$$\bar{j}_i = -\frac{D_i c_i}{kT} \operatorname{grad} \mu_i \Big|_A \qquad (1)$$

$n_{i\alpha}$ is the number of particles of the i-th component in the newly evolving phase, D_i and $\bar{j}_i$ are the partial diffusion coefficient and the density of fluxes of particles at the boundary between both phases, μ_i and c_i are the chemical potential and the volume concentration of the considered component in the medium, A is the surface area of the interface between the two phases, $\bar{e}$ is a unit vector perpendicular to the interface, k the Boltzmann constant and T the absolute temperature.

Restricting ourselves here to the case, that the growth rate is determined by diffusion processes of only one of the components and considering the mixture in the matrix as a perfect one, eqs. (1) yield

$$\frac{dn_\alpha}{dt} = -4\pi A \bar{j} \bar{e}$$

$$\bar{j} = -D \operatorname{grad} c \Big|_A \qquad (2)$$

c, $\bar{j}$, and D being the volume concentration, the density of fluxes and the partial diffusion coefficient of the considered component

in the matrix.

Assuming that D is a constant, the concentration profile in the vicinity of the interface can be determined by the time-dependent diffusion equation

$$\frac{\partial c}{\partial t} = D \Delta c \qquad (3)$$

Thus, we get a set of three equations (2) and (3) for the determination of the growth rate.

2. Growth at Spherical Interfaces

This set of equations (2) and (3) can be simplified if the newly evolving phase has some special type of symmetry. If, e.g., the evolving phase consists of spherical clusters with a constant density ϱ_α and the radius R eqs. (2) and (3) yield

$$\frac{dR}{dt} = - \frac{j(R)}{c_\alpha} \qquad \frac{\partial c}{\partial t} = \frac{D}{r^2} \frac{\partial}{\partial r} \left(r^2 \frac{\partial c}{\partial r}\right)$$
$$j(R) = - D \left.\frac{\partial c}{\partial r}\right|_{r=R} \qquad (4)$$

For small supersaturations the time-derivative $\partial c / \partial t$ can be taken as zero /4/ and the concentration profile around the cluster is given by (see also /5/)

$$c(r) = - \frac{c - c_R}{R} r + c \qquad (5)$$

c and c_R are the concentrations of the segregating particles sufficiently far away from and in the immediate vicinity of the cluster, respectively. Moreover, c_R is determined by the assumption of a local equilibrium in the immediate vicinity of the surface of the cluster.

A substitution of eq. (5) into eq. (4) yields

$$\frac{dR}{dt} = D \frac{c - c_R}{R} \qquad (6)$$

If instead of volume diffusion the growth is limited by other transport mechanisms this equation can be generalized to

$$\frac{dR}{dt} = \frac{D}{R^n} (c - c_R) \qquad (7)$$

where n may have the values n=1 (volume diffusion), n=2 (grain boundary diffusion) and n=3 (diffusion along the dislocation lattice) /4/. For kinetic limited growth we have to replace R^n by a constant of molecular dimensions d_0. This case corresponds to some extent to n=0.

Eqs. (7) are valid for small supersaturations. If this condition is not fulfilled, eqs. (4) have to be solved /6/, which result in more complicated growth laws. E.g., for a given size of a cluster growth and decay may proceed according to different rate equations (see, e.g., /7/).

3. Growth at Cylindrical Interfaces

The time-independent diffusion equation describing systems with cylindrical symmetry reads

$$\frac{1}{r}\frac{\partial}{\partial r}\left(r\frac{\partial c}{\partial r}\right) = 0 \qquad (8)$$

with the general solution

$$c(r) = C_1 \ln r + C_2 \qquad C_1, C_2 \text{ - constants} \qquad (9)$$

While the boundary conditions for r=R remain the same as for spherical interfaces

$$c(r) = c_R \qquad (10)$$

for a determination of the second constant of integration in eq. (9) one has to postulate a certain distance d from the interface, where the concentration reaches its undisturbed value. Thus, if one wants to apply the steady-state approximation for cylindrical interfaces, one has to write

$$c(R+d) = c \qquad (11)$$

resulting in

$$C_1 = \frac{c-c_R}{\ln(1+\frac{d}{R})} \qquad C_2 = c_R - \frac{c-c_R}{\ln(1+\frac{d}{R})} \ln R \qquad (12)$$

Instead of eq. (6) the following growth equation is obtained then

$$\frac{dR}{dt} = \frac{D}{c} \quad \frac{c-c_R}{R \ln(1+\frac{d}{R})} \tag{13}$$

In general, d can be a function of the cluster size or of time, again. Thus, eq. (13) has to be supplemented by an equation for d=d(t), and with the exception of kinetic limited growth, where d is known ($d=d_0$=const.) eq. (13) is strictly speaking, not applicable.

But since the dependence of the growth rate on d is weak ($\sim(\ln(1+d/R))^{-1}$) in a first approximation we expect $R^2 \sim t$, which is verified also by a more rigorous approach /8/.

However, it is necessary to underline, that the steady-state approach is not accurate, in general. Indeed, we want to show, now, that for cylindrical interfaces only for growth processes of the order n=0 this method is theoretically consistent.

4. Application of a General Growth Equation to Growth at Cylindrical Interfaces

In a number of recent publications a general growth equation was derived and discussed, which allows, in particular, also the description of segregation processes at cylindrical interfaces. In general, this equation reads /5,9,13/

$$\frac{dn_\alpha}{dt} = -\frac{Dc}{kT} \quad \frac{A}{d} \quad \frac{\partial \phi}{\partial n_\alpha} \tag{14}$$

n_α describes the number of particles of the segregating component in the newly evolving phase, ϕ is the appropriate thermodynamic potential for the given constraints.

If the pressure and the temperature T are kept constant, ϕ is the Gibbs free energy G expressed by

$$G = n_\alpha \mu_\alpha + n_\beta \mu_\beta + \ldots \tag{15}$$

Since the total number of segregating particles remains constant ($n_t = n_\alpha + n_\beta$), assuming incompressibility of the cluster phase ($n_\alpha = c_\alpha V_\alpha$, V_α - volume of the cluster), we obtain after substitution of eq. (15) into (14)

$$\frac{dV_\alpha}{dt} = \frac{Dc}{c_\alpha kT} \frac{A}{d} (\mu_\beta - \mu_\alpha) \qquad (16)$$

Taking d=R and replacing according to the condition of a local equilibrium $\mu_\alpha = \mu_\beta(c_R)$ for spherical clusters eq. (6) is obtained immediately.

For cylindrical interfaces ($V_\alpha = h\pi R^2$, h is the constant length of the cylinder) eq. (16) yields

$$\frac{dR}{dt} = - \frac{Dc}{c_\alpha kT} \frac{\mu_\alpha - \mu_\beta}{d} \qquad (17)$$

Since, further,

$$\mu_\alpha = \mu_\beta(c_R) = \mu(c^+) + kT \ln \frac{c_R}{c^+}$$
$$\mu_\beta = \mu(c) = \mu(c^+) + kT \ln \frac{c}{c^+} \qquad (18)$$

c^+ being the reference value of the concentration, it follows

$$\mu_\alpha - \mu_\beta = kT \ln \frac{c_R}{c} = kT \ln \frac{c+(c_R-c)}{c} \simeq kT \frac{c_R-c}{c} \qquad (19)$$

and eq. (17) reads

$$\frac{dR}{dt} = \frac{D}{c_\alpha} \frac{c-c_R}{d} \qquad (20)$$

A comparison of eq. (20) with eq. (13) indicates, that both approaches are equivalent for

$$d = R \ln(1+d/R) \qquad (21)$$

or for

$$\ln(1 + \frac{1}{(R/d)})^{R/d} = 1 \qquad (22)$$

This equation is fulfilled strictly only for $d \to 0$. Thus we conclude in agreement with other authors (e.g., /8/) that for cylindrical interfaces the steady-state approach can be, in general, only a more or less accurate approximation. For kinetic limited growth ($d=d_0$, $d_0 \ll R$) this approach remains, however, valid strictly.

5. Growth at Planar Interfaces

For planar interfaces the problems remain the same as discussed in the last paragraph for cylindrical ones. Instead of eqs. (13) and (20) we obtain

$$\frac{dx}{dt} = \frac{D}{c_\alpha} \frac{c-c_x}{d} \qquad (22)$$

and d cannot be determined by a comparison. x in eq. (22) describes the actual position of the interface.

6. Discussion

It was emphasized in the preceding discussions that due to the ambiguities in the determination of the diffusion length d the steady-state approximation cannot be applied, in general, for a description of segregation processes at non-spherical interfaces. However, in a number of practical situations the value of d becomes evident from the particular properties of the system of interest.

If, e.g., a compound (AB) is formed by a solid state reaction of the types of particles A and B at planar interfaces (see Fig. 1, /11/) then d is equal to the width of the already formed compound (AB), being equal to $d=(x_1+|x_2|)$.

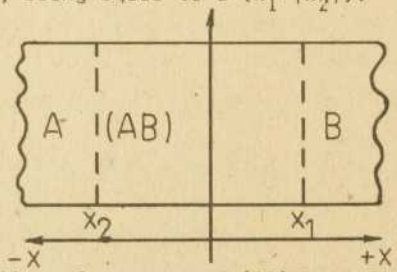

Fig. 1: Formation of a compound (AB) by solid state reactions between A and B particles. A and B are transferred to the reaction sites by diffusion processes.

The rate equations for x_1 and x_2 are given then by

$$\frac{dx_1}{dt} = \frac{D_A}{c_A} \frac{c_A(x_2)-c_A(x_1)}{(x_1+|x_2|)} \qquad \frac{dx_2}{dt} = \frac{D_B}{c_B} \frac{c_B(x_2)-c_B(x_1)}{(x_1+|x_2|)} \qquad (23)$$

$c_A(x)$ and $c_B(x)$ are the volume concentrations of A and B particles, respectively, in the compound (AB) at the position x, D_A and D_B are the diffusion coefficients of A and B-particles in the compound (AB).

Another example is the crystallization of oxygen reduced silica glasses. In this case the diffusion of oxygen from the boundaries is the rate determining step /12/. For a cylindrical body we obtain in this case from eq. (10)

$$\frac{dR}{dt} = \frac{D}{c_\alpha} \frac{c(R)-c(R_1)}{R_1-R} \tag{24}$$

with the solution

$$\frac{d(R_1-R)^2}{dt} = \frac{2D}{c_\alpha} \left[c(R_1)-c(R)\right] \tag{25}$$

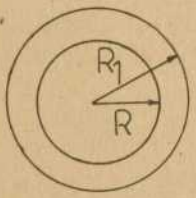

Fig. 2: Crystallization of a cylindrical glass sample by oxygen diffusion from the outer boundaries.

It is evident that the derivation of growth equations for such cases is more straightforward, if one starts with the general equation (14) compared with the diffusion equation approach based on eqs. (2).

Summarizing, we may state that

- the general growth equation (14) is applicable also for the description of growth at non-spherical interfaces
- in a number of situations the direct application of eq. (14) has advantages compared with the diffusion-equation approach
- the effective width d of the inhomogeneous region in the vicinity of the cluster may depend, in general, on time
- the dependence of the growth rate on d is weak for cylindrical interfaces.

References

1. Crank, J.: The Mathematics of Diffusion, Oxford 1975
2. Lifshitz, I.M.; Slyozov, V.V.: J.Exper.Theor.Phys. (USSR) 35 (1958) 479
3. Shewman, P.G.: Diffusion in Solids, Moscow 1966 (in Russian)
4. Slyozov, V.V.; Sagalovich, V.V.: Usp.Fiz.Nauk (USSR) 151 (1987) 67
5. Schmelzer, J.: Thermodynamik finiter Systeme und die Kinetik von thermodynamischen Phasenübergängen 1. Art, Diss. B, Rostock 1985
6. Simmich, O.: Physica Stat.Solidi 173 (1982) 107
7. Aaron, H.B.; Fainstein, D. and Kotter, G.R.: J.Appl Physics 41 (1970) 4404
8. Marqusee, J.A.: J.Chem.Phys. 81 (1984) 976
9. Schmelzer, J.: Z.Phys.Chem. (Leipzig) 266 (1985) 1057
10. Schmelzer, J.; Gutzow, I.: Wiss.Zeitschrift der WPU Rostock NR 35 (1986) 5
11. Blau, W.: Lecture Course "Solid State Reactions", Rostock 1984
12. Rawson, H.: Inorganic Glass-forming Systems, London - New York 1967
13. Ulbricht, H.; Schmelzer, J.; Mahnke, R.; Schweitzer, F.: Thermodynamics of Finite Systems and the Kinetics of First-Order Phase Transitions, Teubner, Leipzig 1988

Author:

Dr. sc. Jürn Schmelzer
Wilhelm-Pieck-Universität Rostock
Sektion Physik
Universitätsplatz 3
Rostock
DDR - 2500

Rostocker Physikalische Manuskripte, Heft 12 (1988)

Wladimir F. Morosow; Heiko Tietze

Helix-Coil Transitions in Solutions

1. Helix and Coil states of the macromolecule

In this paper a chain-like macromolecule consisting of N particles is considered, N being a large number ($N \rightsquigarrow \infty$). For low temperatures hydrogen bonds can be established between the particles leading to an ordered chain with a so-called Helix structure. With an increasing temperature this H-bonds will be breaked and the chain is transformed into a disordered state denoted as a Coil structure (Fig. 1).

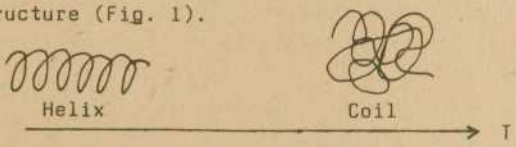

Fig. 1: Helix and Coil state of a chain macromolecule in dependence on temperature T

A reversible transition between the Helix and the Coil states is possible in a certain range of the temperature. It is characterized by a cooperative behaviour of the molecule, that means a transition occurs only if large groups of hydrogen bonds will be formed or breaked off.

This paper deals with an estimation of the critical temperature T_c for the Helix-Coil transition and an investigation of the correlation length which gives a measure for the cooperative behaviour of the system. In particular, we consider natural polypeptides where in the Helix state the H-bonds are established between the j-th and the (j+4)th particles of the chain /1/ (Fig. 2)

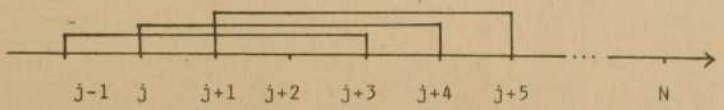

Fig. 2: Model of the Helix state of the polypeptide chain. The brackets indicate the hydrogen bonds

2. Partition function of the chain

The theoretical description of the chain in the Helix state (Fig. 2) is based on the Potts model, which starts with the assumption that every particle of the chain (i=1,...,N) has got $\sigma_i = 1,2,\ldots,$ Q discrete states. Q agrees with the number of possible conformations of every particle in the macromolecule. For Alanin Q is found to be 64, for Glycerine we have Q=32. Denoting the energy of a single hydrogen bond in the chain by U we find for the Hamiltonian of the chain:

$$H = - U \sum_{i=1}^{N} \delta^{(\alpha)}_{\sigma_{i,1}} \qquad (2.1)$$

$\delta^{(\alpha)}_{\sigma_{i,1}}$ is the Kronecker symbol. We have $\delta^{(\alpha)}_{\sigma_{i,1}} = 1$ only if α sequenced particles have the same configuration $\sigma_i = 1$. For natural polypeptides it yields $\alpha = 3$, that means the particles (j+1), (j+2), (j+3) between the jth and the (j+4)th particles must have the same configuration (cf. Fig. 2).

The partition function of the chain can be obtained in the form

$$Z = \sum_{\{\sigma_i\}} \exp\left\{\frac{H}{k_B T}\right\} = \sum_{\{\sigma_i\}} \prod_{i=1}^{N} \left(1 - V \delta^{(\alpha)}_{\sigma_{i,1}}\right) \qquad (2.2)$$

$\{\sigma_i\}$ stands for all possible conformations in the chain, and

$$V = \exp(\beta U) - 1, \quad \beta = 1/k_B T \qquad (2.3)$$

is the known Mayer function. Because the Hamiltonian H (eq. 2.1) can be transformed into a $(Q^{\alpha-1}, Q^{\alpha-1})$ matrix, that is the so-called transfer matrix G, the partition function Z can be expressed also by: $Z = \mathrm{Tr}(G^N)$. A diagonal transformation of the G-matrix leads to:

$$Z = \sum_k \lambda_k^N \qquad (2.4)$$

λ_k being the eigen value of the matrix G. For $N \to \infty$ eq. (2.4) can be approximated by $Z = \lambda^N$, where λ is the largest positive eigenvalue of G.

3. Critical temperature of the Helix-Coil transition

λ can be determined by solving the equation for the eigenvalues:

$$\lambda^{\alpha} - (V + Q)\,\lambda^{\alpha-1} + V(Q + 1)\sum_{h=2}^{\alpha-2}\lambda^{h} = 0 \qquad (3.1)$$

This equation has got α non-trivial eigenvalues. We have solved eq. (3.1) by means of an iteration, starting with the value $\lambda_0 = V + Q$. For low temperatures, that means in the Helix state, V is large compared with Q and we find: $\lambda_0^{low} = V$. In contrast, for high temperatures (Coil state) it yields $\lambda_0^{high} = Q$, because V is small. It seems to be reasonable to approximate the transition between the Helix and the Coil state by:

$$\lambda_0^{low} = \lambda_0^{high} \quad , \quad \text{for } T = T_c \qquad (3.2)$$

From this condition we find for the transition temperature T_c in a first approximation:

$$T_c \simeq U\left(k_B T \ln (1+Q)\right)^{-1} \qquad (3.3)$$

It can be shown that this approximation is valid for every step of the iteration and for any value of α.
The result is summarized in Fig. 3.

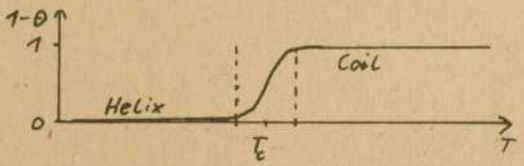

Fig. 3: Degree of spirality θ of the chain in dependence on temperature. T_c is given by eq. (3.3)

The degree of spirality is defined by the ratio of the mean number of hydrogen bonds compared with the number of particles N. If all particles are bound in H-bonds (Helix state) it yields $\theta = 1$.

Fig. 3 demonstrates that the Helix-Coil transition is similar to a diffuse phase transition, because we find a continuous change of the degree of spirality in a certain range of the temperature.

4. Correlation length for the Helix-Coil transition

Now we investigate the correlation function F(r) for two particles of the chain at the distance r. In agreement with experimental experiences we choose the following ansatz for F(r):

$$F(r) = A \exp\{-r/\xi\} \quad (4.1)$$

ξ being the correlation length which gives a measure for the cooperative behaviour. The pre-factor A can be derived from the boundary conditions to be $A = \theta(1-\theta)$. The degree of spirality θ discussed before can be expressed in the form:

$$\theta = \frac{1}{N}\left\langle \sum_{i=1}^{N} \delta_{\sigma_{i,1}}^{(k)} \right\rangle = \frac{V+1}{\lambda}\,\frac{\partial\lambda}{\partial V} \quad (4.2)$$

In the limit of large N we find the following relation between ξ and θ:

$$\coth(1/2\,\xi) \underset{N\to\infty}{=} (V+1)\,\frac{\partial\theta/\partial V}{\theta(1-\theta)} \quad (4.3)$$

Since the number of conformations $Q \gg 1$, and $N \to \infty$ an approximation for the correlation length in the range of the Helix-Coil transition can be derived in the form /3/:

$$\xi_c \sim Q^{(\alpha-1)/2} \quad , \text{ for } T \gtrsim T_c \quad (4.4)$$

This approximation has been confirmed by numerical calculations for Alanin and Glycerine.

5. Modifications of the Helix-Coil transition in the presence of a solvent

If the macromolecule exists in a solvent, hydrogen bonds between the chain and the solvent can be formed in competition to the H-bonds in the chain. These additional bonds depend on the number of unbound particles in the chain (in detail: Amino- and Carboxyl groups) and on the orientation between the solvent molecules and the chain. The orientation between the Amino groups and the solvent molecules is denoted by $p_i = 1,2,\ldots,q$ and between the carboxyl groups and the solvent molecules by $s_i = 1,2,\ldots,q$. Both orientations may have a number q of discrete values. The Hamiltonian of the macromolecule is, now, in contrast to eq. (2.1), given by:

$$H = -\sum_{i=1}^{N} \left[U \delta^{(4)}_{\sigma_{i,1}} + E(1-\delta^{(4)}_{\sigma_{i,1}})(\delta_{s_{i,1}} + \delta_{p_{i,1}}) \right] \qquad (5.1)$$

where E denotes the binding energy of a single H-bond between the chain and the solvent. The partition function Z can be expressed, instead of eq. (2.2), by:

$$Z = (q+W)^{2N} \sum_{\{\sigma_i\}} \prod_{i=1}^{N} (1+\tilde{V}\, \delta^{(4)}_{\sigma_{i,1}}) \qquad (5.2)$$

$\tilde{V}$ means a generalized Mayer function introduced as

$$\tilde{V} = \frac{q^2(1+V)}{(q+W)^2} - 1 \qquad (5.3)$$

with $V = \exp(\beta U)-1$ (eq. 2.3) and $W = \exp(\beta E)-1$ in analogy to V. The pre-factor $(q+W)^{2N}$ is not important for a further calculation of the interesting values T_c and ϱ_c. If it is chosen to be equal to one, we are able to calculate T_c in the same way as discussed in section 3, but now inserting $\tilde{V}$ (eq. 5.3) instead of the former V. Fig. 4 presents the generalized Mayer function $\tilde{V}$ in dependence on the temperature. In order to determine the critical temperature T_c for the Helix-Coil transition in presence of a solvent we use, again, the condition (eq. 3.2) resulting in $\tilde{V}(T)=0$. For this equation two solutions may exist in dependence on the number of conformations Q and on the ratio $\gamma = E/U$ (cf. Fig. 4). For lower values of Q and $E > U/2$ we find two critical temperatures /2/. For this case Fig. 5 presents the modification of the Helix-Coil transition in presence of a solvent in contrast to Fig. 3:

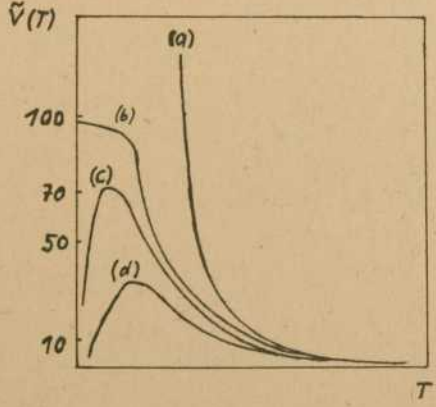

Fig. 4:
V (eq. 5.3) in dependence on the temperature for q = 10 and different values of the ratio $\gamma = E/U$

(a) $\gamma = 0$ (b) $\gamma = 0.5$
(c) $\gamma = 0.51$ (d) $\gamma = 0.52$

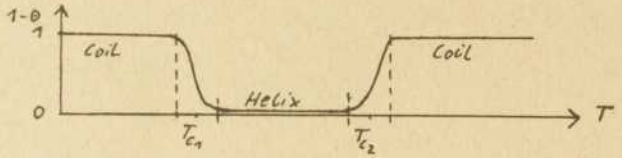

Fig. 5: Degree of spirality θ of the chain in dependence on temperature T in the presence of a solvent

Fig. 5 shows that a Helix state of the macromolecule can exist only between the critical temperatures T_{c1} and T_{c2}. For $T \simeq T_{c1}$ the molecules of the solvent effect an ordered orientation of the particles of the chain, resulting in a transition into the Helix state. At the higher critical temperature T_{c2} the hydrogen bonds will be breaked off again, as discussed before in section 3, and a transition into the coil state occurs. The results for the correlation length in the range of the transition given in section 4 are not modified by the effect of a solvent on the chain.

Acknowledgement

The authors are indebted to Dr. F. Schweitzer for his engagement in preparation and translation of this manuscript.

References

1. Flory, P.J.: Statistical mechanics of chain molecules, Moscow 1971 (in Russian)
2. Morosow, W.F.; Mamasachslisow, E.S.; Ananikjan, N.S.; Atijan, S.A.: Helix-Coil transition in polypeptides - microscopic approach, Jerewan 1987, to be published
3. Tietze, H.: Forschungsbeleg, WPU Rostock 1988

Authors:

Doz. Dr. Wladimir F. Morosow
Staatliche Universität Jerevan
Physikalische Fakultät
Mravian street 1
Jerevan 375049, USSR

stud. phys. Heiko Tietze
Wilhelm-Pieck-Universität Rostock
Sektion Physik
Universitätsplatz 3
Rostock
DDR - 2500

H i n w e i s

Wilhelm-Pieck-Universität Rostock, Sektion Physik (WB IV)

Recent publications on the thermodynamic and kinetic theory of first-order phase transitions:

Schmelzer, J.; Schweitzer, F.: On the Kinetic Description of Condensation in Binary Vapours, Ann. Physik (Leipzig) 44 (1987) 283

Schmelzer, J.; Schweitzer, F.: Ostwald Ripening of Bubbles in Liquid-Gas Solutions, J.Non-Equilib. Thermodyn. 12 (1987) 255

Schmelzer, J.; Ulbricht, H.: Thermodynamics of Finite Systems and the Kinetics of First-Order Phase Transitions, J.Colloid Interface Sci. 117 (1987) 325

Schweitzer, F.; Schimansky-Geier, L.: Critical Parameters for Nucleation in Finite Systems, J.Colloid Interface Sci. 119 (1987) 67

Schmelzer, J.; Schweitzer, F.: Thermodynamics of Heterogeneous Systems: Stability Analysis, Wiss.Z. WPU Rostock N-Reihe 36 (1987) 1, 66

Schweitzer, F.; Tietze, H.: On the nucleation barrier in finite systems: An investigation of the thermodynamic potential, Wiss.Z. WPU Rostock N-Reihe 36 (1987) 1, 17

Mahnke, R.; Budde, A.: Keimbildung in isothermen Systemen, Wiss.Z. WPU Rostock N-Reihe 36 (1987) 1, 50

Budde, A.; Mahnke, R.: Keimbildung unter isoenergetischen Randbedingungen, Wiss.Z. WPU Rostock N-Reihe 36 (1987) 1, 56

Schweitzer, F.; Schimansky-Geier, L.: Stochastic Approach to Nucleation in Finite Systems: Theory and Computer Simulations, Physica A (1988) in press

Schmelzer, J.; Ulbricht, H.: Kinetics of First-Order Phase Transitions in Adiabatic Systems, J.Colloid Interface Sci. (1988) in press

Schmelzer, J.; Schweitzer, F.: Thermodynamics and Nucleation, II. Adiabatic Nucleation in Finite Systems, Z.phys.Chemie (Leipzig) (1988) in press

Schriftenreihen der Wilhelm-Pieck-Universität Rostock

- Archiv der Freunde der Naturgeschichte in Mecklenburg ISSN 0518-3189
- Rostocker Agrarwissenschaftliche Beiträge ISSN 0138-3299
- Rostocker Betriebswirtschaftliche Manuskripte ISSN 0232-3066
- Rostocker Mathematisches Kolloquium ISSN 0138-3248
- Rostocker Philosophische Manuskripte ISSN 0557-3599
- Rostocker Physikalische Manuskripte ISSN 0138-3140
- Rostocker Wissenschaftshistorische Manuskripte ISSN 0138-3191
- Lateinamerika/Semesterbericht der Sektion Lateinamerikawissenschaften ISSN 0458-7944
- Erziehungswissenschaftliche Beiträge ISSN 0138-2373
- Fremdarbeiterpolitik des Imperialismus ISSN 0138-3396
- Beiträge zur Geschichte der Wilhelm-Pieck-Universität Rostock ISSN 0232-539X
- Beiträge zur Geschichte der FDJ ISSN 0233-0830
- Probleme der Agrargeschichte des Feudalismus und des Kapitalismus ISSN 0233-0636
- Rostocker Beiträge zur Hoch- und Fachschulpädagogik ISSN 0233-0539
- Rostocker Informatik-Berichte ISSN 0233-0784
- Studien zur Geschichte der deutsch-polnischen Beziehungen ISSN 0233-0687
- Rostocker Forschungen zur Sprach- und Literaturwissenschaft ISSN 0233-0644
- Rostocker Universitätsreden

Bezugsmöglichkeiten

- Bestellungen aus der DDR über die Wilhelm-Pieck-Universität Rostock, Abt. Wissenschaftspublizistik, Vogelsang 13/14, Rostock, DDR - 2500
- Bestellungen aus dem Ausland über die Firma Buchexport, Volkseigener Außenhandelsbetrieb der DDR, Leninstr. 16, Leipzig, DDR - 7010

Ferner sind die Hefte im Rahmen des Schriftentausches über die Wilhelm-Pieck-Universität Rostock, Universitätsbibliothek, Tauschstelle, Universitätsplatz 5, Rostock, DDR - 2500, zu beziehen.

ikalische Manuskripte, Heft 12 (1988)

Wolfhart Göcke; Winfried Blau

Investigation of Nucleation, Growth and Ripening
.c Glasses

on

e basis of borosilicates containing metal halide
ites are the foundation of the production of photo-
es. The photochromic effect of darkening during ir-
ultraviolet light and fading afterwards is caused
ties of the microcrystallites precipitated in the
o a heat treatment. In some glasses a liquid-liquid
ion of the base glass is necessary in order to pre-
metal halide within the minor phase of the glass.
s investigated here the formation of the metal ha-
s shown to take place without any preceding phase
the glass /1/.
hromic properties of the glasses are strongly in-
he structure properties of the microcrystallites
cture, composition, diameter distribution, phase
r of crystallites per volume (particle density)).
ers can be controlled by the heat treatment of the
Angle X-ray Scattering (SAXS) is an important tool
tigation of the correlations between the conditions
reatment and the structure properties. The results
the optimization of the production process of pho-
sses.

al

nique is very useful in investigating sub-micro-
ition heterogeneities. In particular, the size
the shape, the phase volume, the total inner sur-
particle density of a system of dispersed particles
ined. In the case of phase separation in glasses